UNIVERISTY OF OSLO

MASTER THESIS

Implementing halogen chemistry in the marine boundary layer in the Arctic into the CTM3

Author:
Susanne Foldvik

Supervisor:
Professor Terje Koren Berntsen

Meteorology
Department of Geosciences

August 25, 2017

Abstract

This thesis investigates the ozone depletion event taking place in the marine boundary layer during springtime in the Arctic. The depletion is the result of halogen chemistry, with sources from the ocean in the form of bromocarbons, such as CH_3Br, CH_2Br_2 and $CHBr_3$. The sources supply bromine to the atmosphere, so that the heterogenous reaction at the ice/snow surface with HOBr can take place, creating an bromine explosion. The bromine explosion usually need the help of frost flowers, which provide enough surface area to set off the exponential growth of bromine.

The box model is set up with inital values of bromine, and run for 21 days. The reaction onto aersol surface is calculated using Henry's law, providing a γ function which depends on the mass of HBr and HCl. Then a control run with a boundary layer of 200 meter, at 85.5 °N, starting 1. april, and a β equal to 1.4 is tested. Followed by mulitple experiments: changing the height of the boundary layer from 200 m to 500 m and 1000 m, which loweres the depletion effect. Starting the run at differect times of the year, in June, October and January, where June and October has an increase in depletion, has Januray no depletion. Moving the box to different latitudes, at 45 °N and at the Equator, which decreases the ozone depletion. Varing the surface conditions by changing β to 0.8 and 1.0, which decreases the ozone depletion. And vary the ratio between the R3 and R14 at 60:40 and 70:30, which has a postive effect on the depletion scheme.

Then the CTM3 is set up with only tropospheric chemistry running. The reactions used in the box model is now introduced to the CTM3 model, together with sources from the ocean. Initially, the experiments where suppose to run with emissions multiplied by 1, 10, 100 and 1000, howver, the program is not running properly, so the result is wrong. The result is unrealitic with extremely high values in Bry, Cly and HOBr.

The future plans would be to get the CTM3 model fixed, and model the decrease in ozone levels with and without halogen chemistry, calculating the Radiative Forcing (RF) and the temperature change from pre-industrial times.

Acknowledgements

I would like to thank my supervisor Terje Koren Berntsen for good guidance and cooperation. Without his help this thesis would not have been concluded. A big thank you to Amund Søvde Haslerud from Center for International Climate and Enviromental Research - Oslo (CICERO) for teaching me how to operate the Chemical Transport Model 3 (CTM3) and for good guidance and help. I would also like to thank Anne Claire Fouilloux for helping me with all sort of computer problems. And a big thank you to Bjørg Rognerud for providing me with a matlab program used to plot data from the CTM3.

Contents

Abbreviations

ODE Ozone Depletion Event

MBL Marine Boundary Layer

CTM3 Chemical Transport Model 3

RF Radiative Forcing

VOC Volatile Organic Compounds

NTCF Near-Term Climate Force

CICERO Center for International Climate and Enviromental Research - Oslo

ECMWF European Centre for Medium - Range Weather Forecasts

IFS Integrated Forecast System

SOM Second Order Moment

CCN Cloud Condensation Nuclei

VOC Volatile Organic Compound

PV Potential Vorticity

BC Black Carbon

SW Shortwave

LW Longwave

PBL Planetary Boundary Layer

SLCF Short-Lived Climate Force

BL Boundary Layer

List of Reactions

$$\mathrm{HOBr} + h\nu \longrightarrow \mathrm{Br} + \mathrm{OH} \quad \text{(R1)}$$

$$\mathrm{HOBr} + \mathrm{HBr} \xrightarrow{mp} \mathrm{Br_2} + \mathrm{H_2O} \quad \text{(R2)}$$

$$\mathrm{HOBr} + \mathrm{H^+} + \mathrm{Br^-} \xrightarrow{snow} \mathrm{Br_2} + \mathrm{H_2O} \quad \text{(R3)}$$

$$\mathrm{Br_2} + h\nu \longrightarrow 2\mathrm{Br} \quad \text{(R4)}$$

$$\mathrm{Br} + \mathrm{O_3} \longrightarrow \mathrm{BrO} + \mathrm{O_2} \quad \text{(R5)}$$

$$\mathrm{BrO} + \mathrm{BrO} \longrightarrow 2\mathrm{Br} + \mathrm{O_2} \quad \text{(R6)}$$

$$\mathrm{BrO} + h\nu \longrightarrow \mathrm{Br} + \mathrm{O} \quad \text{(R7)}$$

$$\mathrm{BrO} + \mathrm{HO_2} \longrightarrow \mathrm{HOBr} + \mathrm{O_2} \quad \text{(R8)}$$

$$\mathrm{Br} + \mathrm{HO_2} \longrightarrow \mathrm{HBr} + \mathrm{O_2} \quad \text{(R9)}$$

$$\mathrm{BrO} + \mathrm{NO} \longrightarrow \mathrm{Br} + \mathrm{NO_2} \quad \text{(R10)}$$

$$\mathrm{BrO} + \mathrm{NO_2} + (\mathrm{M}) \longrightarrow \mathrm{BrONO_2} + (\mathrm{M}) \quad \text{(R11)}$$

$$\mathrm{BrONO_2} + \mathrm{H_2O} \xrightarrow{mp} \mathrm{HOBr} + \mathrm{HNO_3} \quad \text{(R12)}$$

$$\mathrm{HOBr} + \mathrm{HCl} \xrightarrow{mp} \mathrm{BrCl} + \mathrm{H_2O} \quad \text{(R13)}$$

$$\mathrm{HOBr} + \mathrm{H^+} + \mathrm{Cl^-} \xrightarrow{snow} \mathrm{BrCl} + \mathrm{H_2O} \quad \text{(R14)}$$

$$\mathrm{BrCl} + h\nu \longrightarrow \mathrm{Br} + \mathrm{Cl} \quad \text{(R15)}$$

$$\mathrm{Cl} + \mathrm{O_3} \longrightarrow \mathrm{ClO} + \mathrm{O_2} \quad \text{(R16)}$$

$$\mathrm{OH} + \mathrm{ClO} \longrightarrow \mathrm{Cl} + \mathrm{HO_2} \quad \text{(R17)}$$

$$\mathrm{OH} + \mathrm{ClO} \longrightarrow \mathrm{HCl} + \mathrm{O_2} \quad \text{(R18)}$$

$$\mathrm{CHBr_3} + \mathrm{OH} \longrightarrow 3\mathrm{Br} + \text{products} \quad \text{(R19)}$$

$$\mathrm{CH_2Br_2} + \mathrm{OH} \longrightarrow 2\mathrm{Br} + \text{products} \quad \text{(R20)}$$

$$\mathrm{CH_3Br} + \mathrm{OH} \longrightarrow \mathrm{Br} + \text{products} \quad \text{(R21)}$$

$$\mathrm{CHBr_3} + h\nu \longrightarrow 3\mathrm{Br} + \text{products} \quad \text{(R22)}$$

$$\mathrm{X_2} + h\nu \longrightarrow 2\mathrm{X} \quad \text{(R23)}$$

$$\mathrm{X} + \mathrm{O_3} \longrightarrow \mathrm{XO} + \mathrm{O_2} \quad \text{(R24)}$$

$$\mathrm{XO} + h\nu \longrightarrow \mathrm{X} + \mathrm{O} \quad \text{(R25)}$$

$$\mathrm{XO} + \mathrm{XO} \longrightarrow \mathrm{X_2} + \mathrm{O_2} \quad \text{(R26)}$$

$$\mathrm{XO} + \mathrm{HO_2} \longrightarrow \mathrm{HOX} + \mathrm{O_2} \quad \text{(R27)}$$

$$\mathrm{HOX} + h\nu \longrightarrow \mathrm{X} + \mathrm{OH} \quad \text{(R28)}$$

$$\mathrm{HOX} + \mathrm{X^-/HX} \xrightarrow{mp} \mathrm{X_2} + \mathrm{OH^-/H_2O} \quad \text{(R29)}$$

Chapter 1

Introduction

1.0.1 Introduction

Studies have shown that the level of tropospheric ozone has increased over the last century (Guicherit et al., 2000, Vingarzan, 2004, Parrish et al., 2009). Since tropospheric ozone is a secondary pollutant from chemical reactions of CO, CH_4 and Volatile Organic Compound (VOC) in the presence of nitrogen oxides (Parrish et al., 2014), an increase in these precursors causes the levels of ozone to rise (Aardenne et al., 2001).

A rise in ozone in the troposphere is concerning for many reasons. Ozone is toxic for human and animals, and contribute to destruction of vegetation (Gillespie et al., 2015; Ainsworth, 2008), and can therefore become a threat to the food security (Debaje, 2014). It is also an important greenhouse gas in the troposphere. IN the context of warming the Arctic, the ozone increase is of concern because ozone also absorbs in short wave radiation in a similar way as Black Carbon (BC) (Monitoring, 2015). BC in the Planetary Boundary Layer (PBL) has a profound warming effect on the surface temperature (Sand et al., 2012, Flanner, 2013), it absorbs the radiation and covers the snow, altering the albedo.

According to the most recent IPCC report, tropospheric ozone has increased with $100 \pm 25\, Tg$ since 1850 (Myhre et al., 2013). The additional ozone added to the troposphere has a profound impact on the Radiative Forcing (RF) (Stevenson et al., 2013). The calculated increase of RF due to ozone since pre-industrial time is $+0.35\ Wm^{-2}$ (0.15 to 0.55), where 0.40 (0.20 to 0.60) Wm^{-2} is tropospheric contribution and -0.05 (-0.15 to 0.05) Wm^{-2} is the stratospheric input (Myhre et al., 2013).

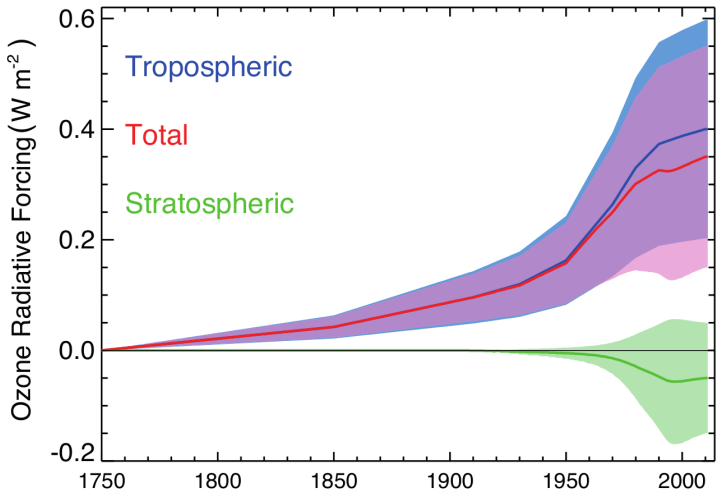

FIGURE 1.1: Evolution of RF due to tropospheric and stratospheric ozone over time (1750-2010). Tropospheric ozone data from (Stevenson et al., 2013), scaled to give $0.40\ Wm^{-2}$ in 2010. Stratospheric data is scaled to give $-0.05\ Wm^{-2}$ in 2010 and follow the Effective Equivalent Stratospheric Chlorine assuming a 3-year gap of air (Daniel et al., 2010). Figure from (Myhre et al., 2013).

Figure 1.1 shows the ozone RF evolution with time, visualizing what was stated above; the total RF contributing from ozone is positive, and is mainly driven by the tropospheric contribution. The reason being that the tropospheric ozone absorb both in the thermal infrared and solar radiation, both contributing positively. Additional ozone around the tropopause creates the greatest positive increase in surface temperature, since the temperature contrast at the tropopause will be the greatest, causing the RF efficiency to be greatest at this point (Lacis et al., 1990, Berntsen et al., 1997). Though in the stratosphere, above about 30 km, the addition of ozone has a negative contribution to the surface temperature, causing local heating which is not reaching the troposphere (Lacis et al., 1990), resulting in a negative RF.

However, the ozone distribution is strongly variable in space and time (Bowman et al., 2013). Its lifetime varies from hours close to polluted areas where its precursors can be found (Monks et al., 2015), up to four months in the free troposphere (Berntsen et al., 1997), with an average of 22 days (Stevenson et al., 2006). This heterogeneity means that the RF contribution of ozone is fluctuating and influenced regionally (Shindell et al., 2009). Ozone also varies seasonally, a maximum in spring to early summer (Vingarzan, 2004). Adding on to variation in latitude and altitude as well (Monks, 2000), ozone is difficult to resolve with many local changes.

To quantify the climate impact of emissions of ozone precursors on Arctic climate, it is probably important to be able to model the ozone distribution not only in the upper troposphere but also in the Boundary Layer (BL). For BC it has been shown absorption of short wave radiation close to ground has a much higher climate efficacy (warming per unit forcing) than if the

absorption takes place higher up (Flanner, 2013). This is because the added heat here triggers local snow/albedo feedbacks. In this thesis it is assumed that this also applies to absorption of short wave radiation by ozone, and thus it is key importance to be able to model ozone close to the surface in order to quantify the climate impact.

A place where such local influences is well illustrated is in the Arctic, where episodes of very low ozone levels are recorded during spring, called an Ozone Depletion Event (ODE) (Bottenheim et al., 1986, Barrie et al., 1988). The events last from several hours to days (Cao et al., 2014), and affects the local RF during this time, as the absorption from ozone won't take place. The ODE can reoccur several times during one season (Martinez et al., 1999), depending on the conditions, such as low temperatures (below $-20\,^{\circ}\mathrm{C}$) and a stable Marine Boundary Layer (MBL) (Simpson et al., 2007). This recurrence will have greater impact on the RF.

The reason for such ODEs are the halogens, with bromine being the strongest depletion agent (Cao et al., 2014). However, most models do not have the halogen chemistry for the troposphere included, and thereby misses the inputs from these events.

The regional impacts from the ODEs give changes to the RF, which in turn translates to a change in temperature (Shindell et al., 2009). As the ODE is being consistent over years, this regional influence could impact the calculated influence from tropospheric ozone in the RF budget (Sherwen et al., 2017). Due to the reduction of ozone, the RF budget might be overestimating the positive change in RF in the polar region in the northern hemisphere.

By adding the halogen chemistry to the Chemical Transport Model 3 (CTM3), the change in O_3 for the Arctic region can be modelled. Using the modelled ozone distribution from the CTM3 the RF can be calculated using either a radiative transfer model or pre-calculated lookup tables from such a model. Following from that a first order estimate of the regional temperature response in the Arctic can be obtained by using a pre-calculated regional temperature coefficient following the methodoly used in Lund et al., 2014 for BC.

The latter calculation of RF and temperature responses is beyond the scope of this thesis, but would be relatively simple once the ozone distribution is properly modelled.

1.0.2 Previous work

Sherwen et al., 2017 has done something similar, where he attemted to calculate the RF by introducing the halogen chemistry. Running the model with preindustrial and present-day emissions, with and without the halogen chemistry, they find a reducion in the RF with the halogens included.

Whereas Sherwen et al., 2017 focuses on the global reduction in RF, this thesis targets the Arctic region only.

1.0.3 Description Of The Thesis

This thesis will focus on finding the key halogen chemistry involved in an ODE, and testing them using a box model. The chemistry will then be inclued in the CTM3, and the change in ozone levels calculated. The aim in then to work out the temperature change, and using a pre-calculated column to calculate the change in RF.

The focus of the thesis is to add the halogen chemistry to the CTM3, calculate the change in RF rising from the ODEs. And from there calculate the difference in temperature from pre-industrial age to present day.

1.0.4 Thesis Introduction

The thesis is organized as follows: the first chapter presents a short background on the radiation and the changes from pre-industrial time, the halogen chemistry and the ODE, and some reaction kinetics. It is followed by a chapter describing the box model and the settings. The results from the box model are presented in Chapter 3, before the CTM3 is introduced and the methodology explained in Chapter 6. In Chapter 7 the results from the CTM3 are presented. The discussion of the results from the two models are in Chapter 5 and 8 together with a conclusion.

Chapter 2

Background Information and Theory

This chapter explains the basic concept of the halogen chemistry leading to an Ozone Depletion Event (ODE) in the Marine Boundary Layer (MBL) (Section 2.1), frost flowers (Section 2.1.3) and the sources of bromine and chlorine (Section 2.1.2. In Section 2.2 the reaction kinetics is explained.

2.1 Halogen Chemistry

Idealized studies such as Berntsen et al., 1997 has shown that for ozone, the Radiative Forcing (RF) from Shortwave (SW) and Longwave (LW) is different depending on the location. In the tropics, most of the absorption happens in the LW spectrum, about 85% of the total RF comes from LW. For latitudes close to the poles, however, about 50% comes from the LW and about 50% from the SW. The halogens are highly photolytical (Simpson et al., 2007), so the extra energy from the sun will help activate the halogen chemsitry.

In order to start the ODE, the key initiation step is the photolysis of dihalogens (Simpson et al., 2007):

$$\mathrm{X_2} + h\nu \longrightarrow 2\mathrm{X} \tag{R23}$$

where the X = I, Br and Cl. The radical X produced by R23 is highly reactive, and will rapidly react with other species, such as ozone:

$$\mathrm{X} + \mathrm{O_3} \longrightarrow \mathrm{XO} + \mathrm{O_2} \tag{R24}$$

XO can then be regenerated by photolysis again:

$$XO + h\nu \longrightarrow X + O \tag{R25}$$

R25 is especially important for X = I and Br, and to a minor extent Cl (Simpson et al., 2007).

The halogen oxides can also react with each other which generally end up destroying ozone by producing a dihalogen which again photolyse with R23:

$$XO + XO \longrightarrow X_2 + O_2 \tag{R26}$$

The halogen oxide can be terminated by reaction:

$$XO + HO_2 \longrightarrow HOX + O_2 \tag{R27}$$

This results in a nonradical reservoir, HOX, which can be reactivated in two important ways. It can be photolysed, R28 or it can react heterogenously with halide anions on or in condenced phases, such as the surface of an aerosol or on snow/ice surfaces, R29 (Simpson et al., 2015):

$$HOX + h\nu \longrightarrow X + OH \tag{R28}$$

$$HOX + X^-/HX \xrightarrow{mp} X_2 + OH^-/H_2O \tag{R29}$$

Because most aqueous systems has the abundance of halide anions in seawater in the order chlorine > bromine > iodine (Simpson et al., 2015), R29 will mostly happen with X^-/HX being Cl^-/HCl, which will produce $BrCl_{aq}$. This dihalogen can react with halides, such as Br^-, often decomposing as Br_2 and Cl^-. This reaction is reversible, but production of gas-phase species that have heavier atoms are favoured, such as I > Br > Cl. Because of low iodine aqueous abundance, production of Br_2 is prefered, even if there is a higher concentration of Cl^- relative to Br^-.

2.1.1 Bromine Explosion

The reactions described above gives a short introduction into the general halogen chemistry, however, it is R29 which really plays a key role in an ODE. This reaction increase the stock of halogen atoms and halogen oxides (X and XO), resulting in a "explosion" which drives the ozone depletion. A particular sequence with bromine, is the main driver of the ODE:

$$\mathrm{HOBr} + \mathrm{Br}^- + \mathrm{H}^+ \xrightarrow{mp} \mathrm{H_2O} + \mathrm{Br_2} \quad \text{(R3)}$$

$$\mathrm{Br_2} + h\nu \longrightarrow 2\mathrm{Br} \quad \text{(R4)}$$

$$\mathrm{Br} + \mathrm{O_3} \longrightarrow \mathrm{BrO} + \mathrm{O_2} \quad \text{(R5)}$$

$$\mathrm{BrO} + \mathrm{HO_2} \longrightarrow \mathrm{HOBr} + \mathrm{O_2} \quad \text{(R8)}$$

The sequence of reactions are known as a "bromine explosion" and is illustrated in Figure 2.1. "mp" is the multiphase reaction, emphasizing the importance of a solution or an ice surface.

The bromine explosion is autocatalytic, so the product is a reactive halogen species, which then acts as a catalyst, speeding up the reaction (Simpson et al., 2007). The sequence consumes one bromine species (HOBr), but returns two reactive bromine species (two Br atoms), which rapidly reacts with ozone, forming BrO. Because of this, there is an exponential growth of BrO concentration in the atmosphere, hence the name "explosion". The large concentration of reactive Br atoms reacting with ozone happens so rapidly that the ozone levels drop drastically, creating the ODE.

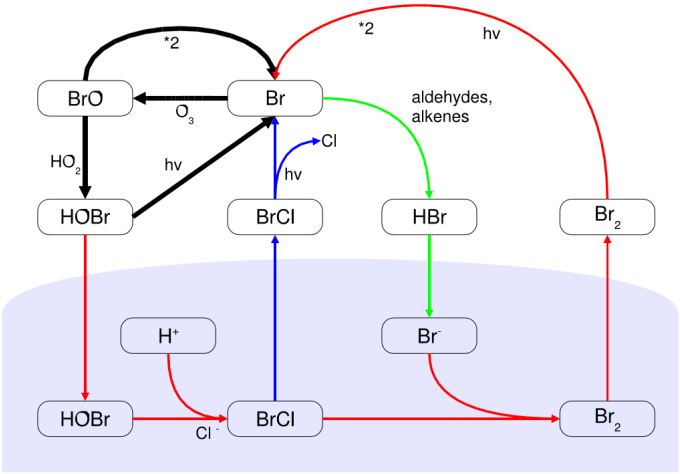

FIGURE 2.1: Bromine explosion reactions in a simplified figure. The blue area represents the condensed phase (liquid brine or the ice surface). The figure is from Simpson et al., 2007

2.1.2 Sources of Halogens

There must be halogens present in the atmosphere in order to activate the halide anions on the snow/ice surface. It must therefore be sources which release halogens into the atmosphere before the R3 and R14 can activate.

It has been shown that sources of halogens include pollution from nocturnal NO_x reservoir that can contribute to chlorine release (Simpson et al., 2015). And that volcanoes salt lakes and lake beds can produce high levels

of halogen oxides linked to mercury chemistry (Simpson et al., 2015). From mountain-top observations, there have also been found sources of IO from the free troposphere (Simpson et al., 2015). However, since it is the bromine explosion which drives the ozone depletion, it is the sources of bromine which are the most interesting ones.

The largest source of bromine- (and iodine-) containing halocarbons comes from the ocean (Ziska et al., 2013). Debromination of sea salt aerosols is the largest source of $\mathrm{Br_y}$ to the troposphere (Parrella et al., 2012). Since the debromination happens in the MBL, the lifetime of $\mathrm{Br_y}$ against depostition is short. The lower the MBL is, the more efficient the debromination is.

However, bromocarbons, such as $\mathrm{CHBr_3}$, $\mathrm{CH2Br_2}$ and $\mathrm{CH_3Br}$ from the marine biosphere, can release $\mathrm{Br_y}$ into the free troposphere, where the lifetime is much longer (Parrella et al., 2012). They are released mainly through the reactions:

$$\mathrm{CHBr_3 + OH \longrightarrow 3Br + products} \quad \text{(R19)}$$

$$\mathrm{CH_2Br_2 + OH \longrightarrow 2Br + products} \quad \text{(R20)}$$

$$\mathrm{CH_3Br + OH \longrightarrow Br + products} \quad \text{(R21)}$$

$$\mathrm{CHBr_3} + h\nu \longrightarrow \mathrm{3Br + products} \quad \text{(R22)}$$

$\mathrm{CH_3Br}$ also has a large anthropogenic source from argicultural pesticide (Parrella et al., 2012). The most dominant precursors of bromocarbons are $\mathrm{CHBr_3}$, $\mathrm{CH_2Br_2}$ (Parrella et al., 2012), released from the oceanic macroalgae and phytoplankton (Quack et al., 2003).

2.1.3 Frost Flowers

Frost flowers are structures growing on a slush layer on a thin, newly formed sea ice in the polar regions. It is formed when brine is brought up to the surface, where it accumulates both as a liquid and as a slush layer (Rankin et al., 2002). The brine evaporates, creating a water vapor layer which is saturated with respect to ice. The structures growing into this layer is enhanced, formed crystals. As the slush layer underneath thickens with saturated brine. Eventualy, the surface tension draws the surface brine onto the frost crystals, creating the frost flowers (Rankin et al., 2002).

Frost flowers has enhanced salinities and about three times more bromine ion concentration compared to that of bulk seawater (Rankin et al., 2002).

Because of the crystal structure, the frost flowers provide a large surface area relative to a flat surface, which enhances the heterogenous reaction R3 and R14. Because of the high bromine ion levels and the large surface area,

R3 can release a lot of Br_2 into the atmosphere in a short period of time, triggering the bromine explosion.

FIGURE 2.2: Frost flowers from 75°58'N 25°34'E, 24 March 2003, with air temperatures around -18 °C. Picture is from Kaleschke et al., 2004.

2.2 Reaction Kinetics

The Chemical Transport Model 3 (CTM3) model will be used, with the chemistry scheme modified to include the halogen chemistry. The reaction rates and the uptake coefficient used in the model will be explained in this section.

2.2.1 Bimolecular Reactions

Most of the reactions considered here are so called *bimolecular* reactions, where reactants A and B give the resultants C and D (Jacob, 1999).:

$$\mathrm{A} + \mathrm{B} \longrightarrow \mathrm{C} + \mathrm{D}$$

The production rate is then calculated as:

$$\frac{d[C]}{dt} = \frac{d[D]}{dt} = \frac{-d[A]}{dt} = \frac{-d[B]}{dt} = k[A][B] \tag{2.1}$$

The concentration [X] refer to the number densities of the species, often with the unit $molecule cm^{-3}$, since the rate constant, which denotes the frequency at which the molecules collide and a reaction takes place, is given in $molecules^{-1}s^{-1}$.

If the reactants are equal, it is still a bimolecular reaction, but is referred to as a *self-reaction* (Jacob, 1999):

$$\mathrm{A} + \mathrm{A} \longrightarrow \mathrm{C} + \mathrm{D}$$

And the rate would look like:

$$\frac{d[C]}{dt} = \frac{d[D]}{dt} = \frac{-d[A]}{dt} = k[A]^2 \tag{2.2}$$

With the units being the same as stated above. The new reactions stated in Table 3.2 use this method for calculating the reaction rate, with the exception of the photolysis and reactions R3 and R14.

2.2.2 Rate of The Downward/Upward Rate From Snow With HOBr

For reactions R3 and R14, the rate is calculated:

$$\frac{d[HOBr]}{dt} = -k_d[HOBr] \tag{2.3}$$

where:

$$k_d = \frac{v_d}{L_{mix}}\beta \tag{2.4}$$

L_{mix} is the typical height of the stable boundary layer. β is the total realtive surface area offered by the snow/ice. If the surface is flat, β is one.

It is assumed that whatever HOBr which deposit onto the ground, all is used up to fuel either R3 or R14. The ratio $\frac{k_{Br}}{k_{Cl}}$ varies between 0.8 and 1.4 (Foster et al., 2001).

v_d is the deposition velocity at the snow/ice surface. Following Seinfeld John, 1988, v_d can be expressed as the sum of three resistances:

$$v_d = (\frac{1}{r_a} + \frac{1}{r_b} + \frac{1}{r_c}) \tag{2.5}$$

r_a is the aerodynamic resistance, r_b is the quasi-laminar layer resistance, and r_c is the surface resistance. r_a is the resistance due to the aerodynamic transport when bringing the gas down to the surface. It is approximated by:

$$r_a \approx \frac{1}{u\kappa^2}\Big(ln(\frac{z}{z_0})\Big)^2$$

κ is the Karman constant, u is the wind speed, z is the height of the surface layer, which is 10% of the boundary layer, so $z = 0.10 \times L_{mix}$. z_0 is the surface roughness length, taken to be constant for ice surface, 10^{-5}m (Huff

et al., 2000, Huff et al., 2002). The wind speed is set to $8\ ms^{-1}$ (Beare et al., 2006), while κ is set to 0.4 (Huff et al., 2000, Huff et al., 2002). Since the local wind speed is constant, r_a depends on the height of the Boundary Layer (BL).

r_b is the resistance due to molecular diffusion to transfer the gas-phase reactant across a liquid-laminar layer above the surface (Cao et al., 2014). It is expressed as:

$$r_b = \frac{z_0}{D_g}$$

z_0 is as stated above, D_g is the molecular diffusivity in gas phase.

r_c is the resistance to loss of the gas-phase reactant at the ice surface. r_c is calculated:

$$r_c = \frac{4}{\upsilon_{therm}\gamma}$$

υ_{therm} is definded further down, in Section 2.2.3. γ is set to 0.06, and this includes the assumption that H^+ and the halogen ions are inexhaustible at the ice/snow surface (Cao et al., 2014).

The ratio $\frac{k_{R3}}{k_{R14}}$ is taken be unity, meaning that of the HOBr depositied onto the snow, half will go to feed reaction R3, and half will go to reaction R14. The ratio varies between 0.8 and 1.4 (Cao et al., 2014), so it is set to a constant.

2.2.3 Uptake Coefficient and Henry's Law

Reactions R2 and R13 are heterogeneous reaction with aerosols, and the rate of reaction must be expressed in a different way. It is not only the gasous concentration that must be represented, but also the reactant suspended in the aerosols (Cao et al., 2014). It is mass dependent, so more mass implies a faster reaction. Looking at R2:

$$HOBr + HBr \xrightarrow{mp} Br_2 + H_2O \tag{R2}$$

The rate of formation is represented as (Schwartz, 1986):

$$\frac{d[Br_2]}{dt} = -\frac{d[HOBr]}{dt} = k_{R2}[HOBr] \tag{2.6}$$

where the k_{R2} is the first order heterogenous reaction-rate constant, expressed as:

$$k_{R2} = (\frac{a}{D_g} + \frac{4}{\upsilon_{therm}\gamma})^{-1}\alpha_{eff} \tag{2.7}$$

D_g is the molecular diffusivity in gas phase, as described in Section 2.2.2, a is the aerosol radius. υ_{therm} is the molecular speed of HOBr, expressed as:

$$\upsilon_{therm} = \sqrt{\frac{8RT}{\pi M_{HOBr}}} \tag{2.8}$$

with R being the universal gas constant, T the absolute temperature and M_{HOBr} is the molar mass of HOBr.
α_{eff} is the surface-volume coefficient:

$$\alpha_{eff} = \frac{A_{aerosol}}{V_{grid-box}} \tag{2.9}$$

γ is the uptake coefficient, in this case for HOBr. γ is defined as *"the net probability that a molecule X undergoing a gas-kinetic collision with a surface is actually taken up at the surface"* (Crowley et al., 2010). Follwing the same resonment, γ is not constant. It is often time dependent, as the number of reactants at the surface change, the solubility may differ and γ depends on the gas phase concentration of the molecule X (Crowley et al., 2010). Described by Hanson et al., 1994, it can be expressed as:

$$\frac{1}{\gamma} = \frac{1}{\alpha} + \frac{\upsilon_{therm}}{4H^*RTf(q)\sqrt{k^I_{liq}D_{liq}}} \tag{2.10}$$

α is the accommodation coefficient, D_{liq} is the HOBr liquid diffusion coefficient, and R, T and υ_{therm} are as described above. H^* is the effective Henry constant, which is applied for species which can dissociate in liquid solutions (Cao et al., 2014), in this case HOBr.

$f(q)$ is a function defined as:

$$f(q) = coth(q) - (\frac{1}{q})$$

$$q = a\sqrt{\frac{k^I_{liq}}{D_{liq}}}$$

$$k^I_{liq} = k^{II}_{liq}[HBr]_{liq} = k^{II}_{liq} H^*_{HBr} P_{HBr}$$

a and D_{liq} are described above, while k^I_{liq} is the first order liquid reaction rate constant. k^{II}_{liq} is the second order liquid reaction rate, H^*_{HBr} is Henry's constant for HBr, for reaction R2. It will be similar for reaction R13, but with HCl instead. P_{HBr} is the partial pressure of gasous HBr + HOBr.

Table 3.6 describes the coefficients mentioned here.

In order to calculate the partial pressure, the ideal gas law is used:

$$pV = nRT \tag{2.11}$$

With p being the total pressure, V is the volume of the air, n is the number of moles of air, while R and T is the universal gas constant and the temperature, respectively. Substituting and rearrangement will give (må nok skrive ligningane litt annerledes):

Substituing $n_a = \frac{A_v n}{V}$ into $p = \frac{nRT}{V}$ will give:

$$p = \frac{n_a RT}{A_v}$$

Substituting this again with $n_x = c_x n_a$ gives:

$$p = \frac{n_x}{c_x}\frac{RT}{A_v}$$

n_a is the number density of air, usually with units in $molecules\ cm^{-3}$, A_v is Avogadro's number, $6.0022 \times 10^{23}\ molecules\ mol^{-1}$ and c_x is the mixing ratio of gas x. After substituting:

$$p = \frac{n_x}{c_x}\frac{RT}{A_v} \tag{2.12}$$

Dalton's law states that the partial pressure of gas x in a mixture of gases is equal to pressure gas x would have exerted if all the other gases were

removed (Jacob, 1999). It is expressed as the mixing ratio c_x of gas x mulitplied by the total pressure:

$$p_x = c_x p \tag{2.13}$$

Inserting this into equation 2.12 gives:

$$p_x = n_x \frac{RT}{A_v} \tag{2.14}$$

Equation 2.14 is used in the box model and in the CTM3 in order to calculate the reaction rate of reactions R2, R13 and R12, described in Section 3.2.4.

All the components are now known, and the rate can be calculated. Table 3.6 lists the values of all the variables used.

Chapter 3

Box Model and Setup

This chapter describes the box model used in this study (Section 3.1), the setup, modifications, and input data (Section 3.2) Descriptions of the experiments are listed in Section 3.3.

3.1 Model Description

Before using the full chemistry transport model, a box model is used to test the scheme with new reactions leading to an Ozone Depletion Event (ODE) and analyze the conditions needed, in addition to doing simple experiments before applying it to the Chemical Transport Model 3 (CTM3). The box model used in this master thesis is built in matlab R2016a. It uses an ordinary differential equation solver to calculate the change in mass. The ordinary differential equation solver used here is ode23t, which gives a solution without numerical damping (from, 2017).

The box model was developed to be used in the course *Regional and global air pollution (GEF2210)* at the University of Oslo. It has some standard chemistry included, such as NOx, CO, HOx and Volatile Organic Compound (VOC) processes, but no bromine and chlorine.

The reactions chosen to be included are based on the box model from Cao et al., 2014 and from Simpson et al., 2015. There are three sections, one for bromine, which is the most important one, as it contains the "bromine explosion" which drives the ODE. Then there is a small section with nitrogen included, with R12 being the most important for the NOx cycle during the ODE (Cao et al., 2014), and one section with chlorine. The chlorine is found to contribute very little, only about 1% of ozone is depleted by chlorine (Cao et al., 2014). However, it is important in processing of the VOC and influences bromine chemistry through BrCl (Simpson et al., 2007), and is therefore included. The reactions are listed in Table 3.2.

3.2 Setup and Modifications

3.2.1 Fixed Conditions

The reaction rate is updated 480 times during 24 hours, meaning every third minute, and the experiments are run for 21 days. The start-day is set to 1st of April (changed in some of the experiments), with a constant temperature at 258K, same as in Cao et al., 2014. The latitude used for the experiments is 85.5°N, with the exception of the model runs where the box is moved to lower latitudes, at 45.0°N, and at the Equator. All emissions from HC, NO, CO is set to zero in order to closer simulate the Arctic environment, and to isolate the ODE. β is set to 1.4 in order to include the simulation of frost flowers, which offers a large surface area due to its sharp angles (Rankin et al., 2002) and is thought to support to the ODE by providing sources from the water (Shaw et al., 2010). The ratio between R3 and R14 is set to fifty-fifty, so out of the deposited HOBr, half will fuel R3 and half will fuel R14.

3.2.2 Reaction Rates

The reaction rate is found by solving equation 2.1 and 2.2 from Chapter 2. Reactions R2, R12 and R13 are calculated as described in Section 3.2.4. Reactions R14 and R3 are described in Section 2.2.2. The expression and coefficients used in the model are listed in Table 3.2.

TABLE 3.1: Halogen chemistry added to the scheme

Reaction	Reaction No.
$HOBr + h\nu \longrightarrow Br + OH$	R1
$HOBr + HBr \xrightarrow{mp} Br_2 + H_2O$	R2
$HOBr + H^+ + Br^- \xrightarrow{snow} Br_2 + H_2O$	R3
$Br_2 + h\nu \longrightarrow 2Br$	R4
$Br + O_3 \longrightarrow BrO + O_2$	R5
$BrO + BrO \longrightarrow 2Br + O_2$	R6
$BrO + h\nu \longrightarrow Br + O$	R7
$BrO + HO_2 \longrightarrow HOBr + O_2$	R8
$Br + HO_2 \longrightarrow HBr + O_2$	R9
$BrO + NO \longrightarrow Br + NO_2$	R10
$BrO + NO_2 + (M) \longrightarrow BrONO_2 + (M)$	R11
$BrONO_2 + H_2O \xrightarrow{mp} HOBr + HNO_3$	R12
$HOBr + HCl \xrightarrow{mp} BrCl + H_2O$	R13
$HOBr + H^+ + Cl^- \xrightarrow{snow} BrCl + H_2O$	R14
$BrCl + h\nu \longrightarrow Br + Cl$	R15
$Cl + O_3 \longrightarrow ClO + O_2$	R16
$OH + ClO \longrightarrow Cl + HO_2$	R17
$OH + ClO \longrightarrow HCl + O_2$	R18

3.2.3 Photolysis

Solar Declination Angle

A function, named delta, is used to calculate the solar declination angle, the latitude where the sun is directly overhead at noon. It varies between $-23.45°$and $+23.45°$over the year, being zero at spring and autumn equinox.

TABLE 3.2: Chemical reactions and rate constants added to the box model, temperature in Kelvin

Reaction No.	Rate Constant	Unit	Reference
R1	see Table 3.4	s^{-1}	(Cao et al., 2014)
R2	see Section 3.2.4	-	(Cao et al., 2014)
R3	$\frac{V_d}{L_{mix}}\beta$	s^{-1}	(Cao et al., 2014)
R4	see Table 3.4	s^{-1}	(Cao et al., 2014)
R5	$1.75 \times 10^{-11} \exp(\frac{-800}{T})$	$cm^3\ molecules^{-1}\ s^{-1}$	(Sander et al., 2006)
R6	$2.4 \times 10^{-12} \exp(\frac{40}{T})$	$cm^3\ molecules^{-1}\ s^{-1}$	(Sander et al., 2006)
R7	see Table 3.4	s^{-1}	(Cao et al., 2014)
R8	$4.5 \times 10^{-12} exp(\frac{460}{T})$	$cm^3\ molecules^{-1}\ s^{-1}$	(Sander et al., 2006)
R9	$4.8 \times 10^{-12} \exp(\frac{-310}{T})$	$cm^3\ molecules^{-1}\ s^{-1}$	(Sander et al., 2006)
R10	$8.8 \times 10^{-12} \exp(\frac{260}{T})$	$cm^3\ molecules^{-1}\ s^{-1}$	(Sander et al., 2006)
R11	3.89×10^{-12}	$cm^3\ molecules^{-1}\ s^{-1}$	(Sander et al., 2006)
R12	see Section 3.2.4	-	(Cao et al., 2014)
R13	see Section 3.2.4	-	(Cao et al., 2014)
R14	$\frac{V_d}{L_{mix}}\beta$	s^{-1}	(Cao et al., 2014)
R15	see Table 3.4	s^{-1}	(Cao et al., 2014)
R16	$2.3 \times 10^{-11} \exp(\frac{-200}{T})$	$cm^3\ molecules^{-1}\ s^{-1}$	(Sander et al., 2006)
R17	$7.4 \times 10^{-12} \exp(\frac{270}{T})$	$cm^3\ molecules^{-1}\ s^{-1}$	(Sander et al., 2006)
R18	$6.0 \times 10^{-13} \exp(\frac{230}{T})$	$cm^3\ molecules^{-1}\ s^{-1}$	(Sander et al., 2006)

Here a third degree Fourier expansion is used (Hartmann, 1994):

$$\delta = \sum_{n=0}^{3} a_n cos(n\theta_d) + b_n sin(n\theta_d) \tag{3.1}$$

The coefficients a_n and b_n are given in Table 3.3 (Hartmann, 1994). The θ_d is the time of the year expressed in radians, calculated by using the formula:

$$\theta_d = \frac{2\pi d_m}{365} \tag{3.2}$$

Where d_m is day number, starting with January 1st as 0 and ending on December 31st on 364.

TABLE 3.3: Coefficients for the delta-function (Hartmann, 1994)

n	a_n	b_n
0	0.006918	-
1	-0.399912	0.070257
2	-0.006758	0.000907
3	-0.002697	0.001480

Photolysis Rate

The photolysis rates are calculated in two different ways, one is with a formula from the emep-website, given here, while the other is taken from Cao et al., 2014. The two methods are used as each of them alone miss some components included in the other. In order to get a photolysis of all the reactions, two methods must be used.

The first method uses the equation:

$$J = JL * cos(z)^{JM} * \exp(\frac{-JN}{cos(z)}) \tag{3.3}$$

Where JL, JM and JN are coefficients listed in Table 3.5, z is the solar zenith angle found by solving the equation (Hartmann, 1994):

$$cos(z) = sin(\phi)sin(\delta) + cos(\phi)cos(\delta)cos(h) \tag{3.4}$$

Where δ is the declination angle, ϕ is the latitude and h is the hour angle. Solving it gives:

$$z = cos^{-1}(sin(\phi)sin(\delta) + cos(\phi)cos(\delta)cos(h)) \tag{3.5}$$

Where the angles are given in degrees.

The second method uses an approach based on earlier models (Röth, 1992; Röth, 2002):

$$J = J_0 * \exp(b[1 - sec(c * z)]) \tag{3.6}$$

The coefficients for J_0, b and c are listed in Table 3.4. The solar zenith angle z is calculated the same way as shown in equation 3.5.

TABLE 3.4: Coefficients used for photolysis rates (Cao et al., 2014)

Species	$J_0[s^{-1}]$	b	c
HOBr	2.62×10^{-3}	1.216	0.861
Br_2	1.07×10^{-1}	0.734	0.900
BrO	1.27×10^{-1}	1.290	0.857
BrCl	3.41×10^{-2}	0.871	0.887
O_3	6.85×10^{-5}	3.510	0.820
NO_2	2.62×10^{-2}	1.068	0.871
H_2O_2	2.75×10^{-5}	1.595	0.848
HNO_3	1.39×10^{-6}	2.094	0.848
NO_3	6.20×10^{-1}	0.608	0.915

TABLE 3.5: Coefficients used for photolysis rate (Röth, 2002)

Species	JL	JM	JN
HCHO	4.87×10^{-5}	0.781	0.343
N_2O_5	3.32×10^{-5}	0.000	0.566

3.2.4 Reaction Rate for Multiphase Reactions

There are three equations that require special attention:

$$HOBr + HBr \xrightarrow{mp} Br_2 + H_2O \tag{R2}$$

$$HOBr + HCl \xrightarrow{mp} BrCl + H_2O \tag{R13}$$

$$BrONO_2 + H_2O \xrightarrow{mp} HOBr + HNO_3 \tag{R12}$$

These are heterogeneous reactions at the surface of the aerosols. For reaction R2, the limiting factor is not only the absorption of the gaseous HOBr, but also the concentration of HBr in the suspended aerosol particles (Cao et al., 2014). This is described in more detail in Section 2.2.3. In the model, equation 2.7 is used to calculate the reaction-rate constant. Table 3.6 shows the coefficients used in the box model.

Reaction R12 is represented for reactions with aerosols, but not with reactions with the snow. Unlike the other two reactions, the uptake coefficient, γ, is set to be 0.06 for reaction R12. Following Cao et al., 2014, the uptake coefficient were set to three different values. With γ equal to 0.0001, the reaction R12 became neglectible, so that less HOBr was formed from nitrogen-containing species. The ODE was therefore slowed down. At $\gamma = 0.06$, the NOx chemistry enhanced the ODE, so it would happen earlier than it would without the nitrogen-cycle. If $\gamma = 0.0004$, the ozone produced by the NOx-cycle would compensate for the ozone depleted by the halogens, and the time it takes for an ODE to happen would be equal to the case without the nitrogen-cycle.

Here, the uptake coefficient was set to 0.06, since the NOx chemistry will tend to enhance the ODE (Cao et al., 2014), and setting it to a dominant value would then increase the chance of getting an ODE.

3.2.5 Sources of halogens

In the box model the halogens are initialized as a constant, listed in Table A.1, and then allowed to grow with new inputs from the snowpack, with unlimited sources of Br^- and Cl^-. There are no sources for halogens from the sea, which would be the case in nature. Since the box-model is used to analyse the reactions and understand the process of an ODE, the sources were simplified. In the global model, however, sources of halogens were included.

3.3 Experiments

In order to investigate and learn more about the behaviour and the dependence on different parameters, mulitple experiments are run:

- The height of the stable Boundary Layer (BL) is changed, this also implies altering in the fallspeed of HOBr towards the snow, seen in Table 3.8.
- The seasonality is tested by starting the run at different times of the year. The run still only lasts 21 days, so it is not really a season, but a small representative for that time of the year.
- The box is moved to 45.0°N and to the Equator, to see how this affects the chemistry.
- β is changed. β simulates the area available for realease of Cl^- and Br^- from the snow. The bigger β is, the more ice/snow surface is available. When frost flowers occur, β will increase, speeding up the heterogenous reactions R3 and R14, accelerating the ODE, explained in 2.1.3.

- The ratio between R3 and R14 so the effectiveness of the sources from the snow is changed. (See Section 2.2.2)

TABLE 3.6: Coefficients used for calculating the rates for multiphase reactions

Name	Explanation	Coefficient	Unit
	HOBr		
α	Accomodation coefficient	1.0	Dimensionless
α_{eff}	Surface-volume coefficient	1.0×10^{-6}	$cm^2/cm{-}3$
a	Aerosol radius	0.45×10^{-4}	cm
D_g	Molecular diffusivity (gas)	0.2	$cm^2 s^{-1}$
M_{HOBr}	Molar mass of HOBr	96.91×10^{-3}	$kg\ mol^{-1}$
D_{liq}	Liquid diffusivity coefficient	5.0×10^{-6}	$cm^2\ s^{-1}$
H^*_{HOBr}	Effective Henry constant (HOBr)	1.7×10^4	$mol\ L^{-1}\ atm^{-1}$
β	Ratio of total relative surface area of the snow/ice and the flat surface	See Section 2.2.2	Dimensionless
	HBr		
H^*_{HBr}	Effective Henry contant (HBr)	3×10^8	$mol\ L^{-1}\ atm^{-1}$
$k^{II}_{liq.HBr}$	Second order liquid reaction rate (HBr)	5.0×10^4	$L\ mol^{-1}\ s^{-1}$
	HCl		
H^*_{HCl}	Effective Henry contant (HCl)	3×10^6	$mol\ L^{-1}\ atm^{-1}$
$k^{II}_{liq.HCl}$	Second order liquid reaction rate (HCl)	10^5	$L\ mol^{-1}\ s^{-1}$
	$BrONO_2$		
γ	Uptake coefficient (for R12)	0.06	Dimensionless

TABLE 3.7: Experiments done with the box model

Name	Height of the stable BL, L_{mix} [m]	Latitude [°N]	Start day	Beta (β)	Ratio R3:R14
BoxControl	200	85.5	1. April	1.4	50:50
BoxBL500	500	85.5	1. April	1.4	50:50
BoxBL1000	1000	85.5	1. April	1.4	50:50
BoxJJA	200	85.5	1. June	1.4	50:50
BoxSON	200	85.5	1. October	1.4	50:50
BoxDJF	200	85.5	1. January	1.4	50:50
BoxLat45	200	45.0	1. April	1.4	50:50
BoxLatEq	200	Equator	1. April	1.4	50:50
BoxBeta0.8	200	85.5	1. April	0.8	50:50
BoxBeta1.0	200	85.5	1. April	1.0	50:50
BoxRatio6040	200	85.5	1. April	1.4	60:40
BoxRatio7030	200	85.5	1. April	1.4	70:30

TABLE 3.8: Deposition velocities for different BL heights

Height of the stable BL, L_{mix} $[m]$	Deposition velocity, v_d $[cms^{-1}]$
200	0.605
500	0.536
1000	0.491

Chapter 4

Results Box model

4.1 Results

In this Chapter, the results from the experiments with the box model are presented. The plots visualize the Ozone Depletion Event (ODE) over the course of 21 days. All the plots show the ozone values on the left hand side, in ppb, while the right hand side shows the halogens, in ppt.

4.1.1 Control Experiment

The control experiment, described in Section 3.3. Looking at Figure 4.1, the ozone drops by 21 ppb from starting point, while the total amount of bromine goes up. There is a steep, continuous rise i BrO in an almost exponential manner, mimiced by the steady rise in the total amount of bromine. A clear sign of an bromine explosion. At the same time, there is a continuous drop in ozone. This is due to reaction R5. Br is also increasing, due to reactions R1, R4, R6, R10 and R15. The HOBr is increasing, then decreasing, as it is transformed into BrO, and Br-molecules.

Notice that the total amount of Br-molecules and Cl-molecules (seen in Figure 4.2) are constantly rising. This is due to the unlimited source of Br^- and Cl^- from the snow.

In Figure4.2 the same experiment is shown, but now with the daily levels of chlorine. The level of ClO is rising, due to R16. Shown by the total amount of Cl-molecules, nearly all is in the form of ClO. This emphasize the importance of the photolysis of R15. However, as stated before, the main depletion of ozone is driven by bromine.

Since bromine is the main driver behind the ODE, this is the focus for the rest of the chapter. Therefore the plots displaying the chlorine are presented in A.

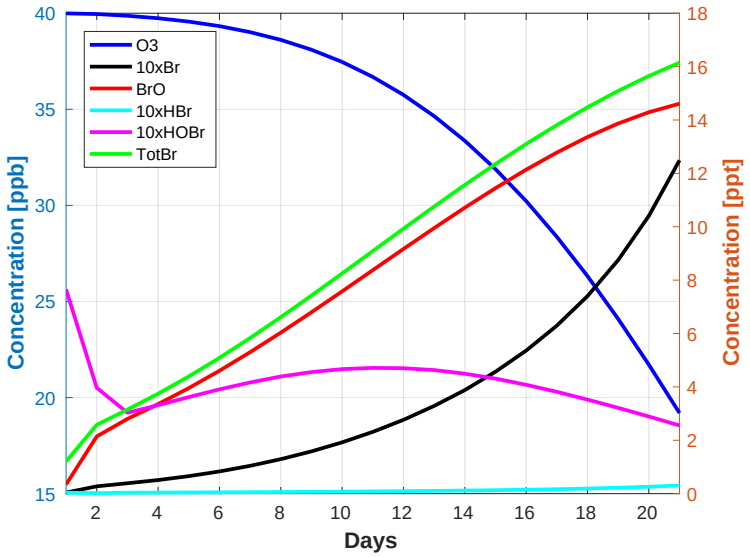

FIGURE 4.1: BoxControl: Daily averages for O_3 (blue), $10 \times$ Br (black), BrO (red), $10 \times$ HBr (cyan), $10 \times$ HOBr (pink) and the total bromine molecules (green) over the course of 21 days.

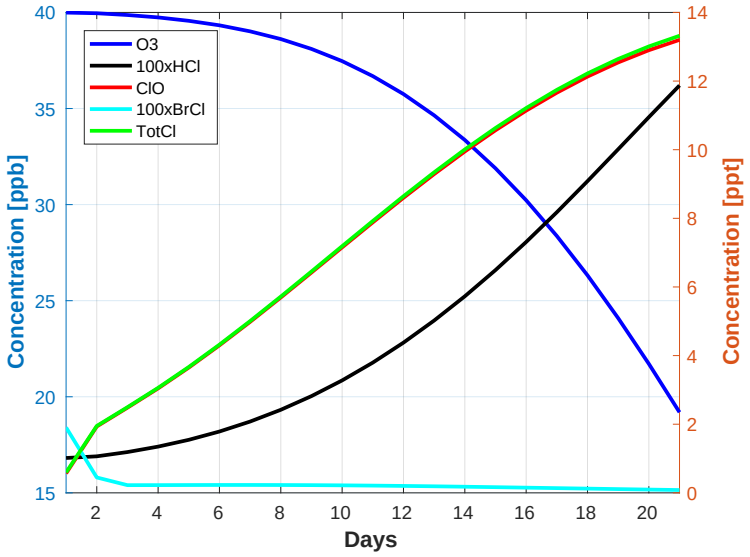

FIGURE 4.2: BoxControl: Daily averages for O_3 (blue), $10 \times$ Br (black), BrO (red), $10 \times$ HBr (cyan), $10 \times$ HOBr (pink) and the total bromine molecules (green) over the course of 21 days.

4.1.2 Changing the Height of the Stable Boundary Layer

The stable boundary layer is changed from 200 meters to 500 meters and 1000 meters, following the experiments done in Cao et al., 2014. Figures 4.3 and 4.4 both show a very small decrease in the ozone levels, however, it not even close to being an ODE. The importance of BrO in the total amount of bromine is still dominating, but now HOBr is more present os well, indicating that the depostion onto the snow is changed.

That the depostion onto the snow changes with changing height of the stable Boundary Layer (BL) is no surprise, as the thickness of the BL is a key component in the ODE. With a more shallow BL, the dilution of the emissions of reactive halogens from the surface is less and since the formation of Br/BrO Cl/ClO is non-linear, the catalytic ozone depletion is expected to be much less effective in deeper BLs.

This is clearly illustrated in Figures 4.3 and 4.4. When the height of the BL was 500 meters, the ozone dropped with 21 ppb, with a height of 500 meters, the drop is 2.5 ppb and with a BL of 1000 meters, the drop is only 0.7 ppb.

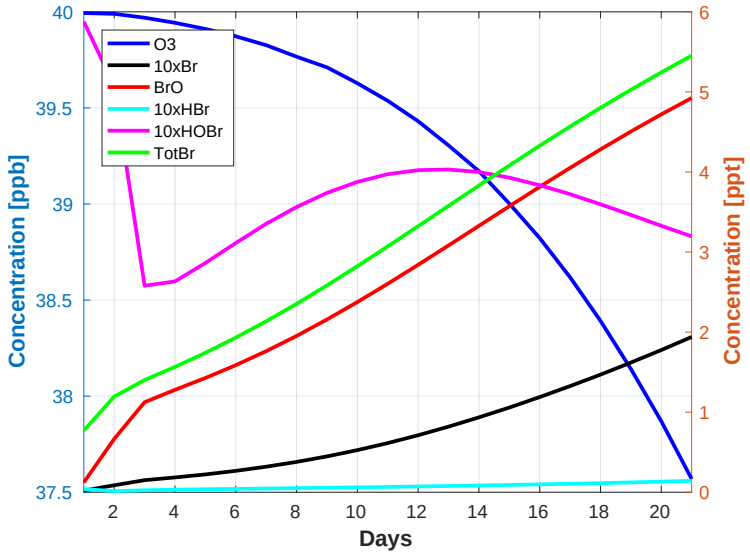

FIGURE 4.3: BoxBL500: Daily averages for O_3, $10 \times$ Br, BrO, $10 \times$ HBr, $10 \times$ HOBr and the total bromine molecules.

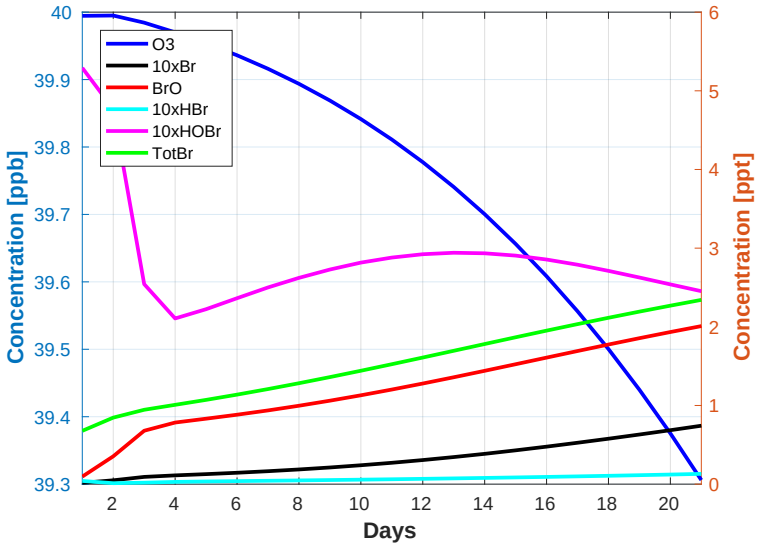

FIGURE 4.4: BoxBL1000: Daily averages for O_3, $100 \times HCl$, ClO, $100 \times BrCl$ and the total chlorine molecules over the course of 21 days.

4.1.3 Seasonal Variation

The control experiment starts 1. april. Now the model is set to start in 1st of June, 1st of October and 1st of January, and then run for 21 days.

In the summer, when the experiment start the 1st of June, Figure 4.5, the sun will never set and the breakdown of ozone will continue. Due to the midnight sun, the depletion is more efficient than in the control experiment, which represents the spring, shown in Figure 4.1.

Figure 4.7 shows the results for the experiment starting the 1st of Januray, and there is almost no effect on the ozone levels. This is due to the sun being below the horizon, limiting the photolysis, preventing the activation of bromine and surpressing the ODE.

In Figure 4.6, starting the 1st of October, the sun is still up, making photolysis possible, driving the ODE.

There is a more efficient depletion in the summer, BoxJJA, with ozone levels dropping 26 ppb. The same is the case for the autumn, BoxSON, where ozone drops by 26.5 ppb. The winter season, BoxDJF, shows only a drop in 0.05 ppb.

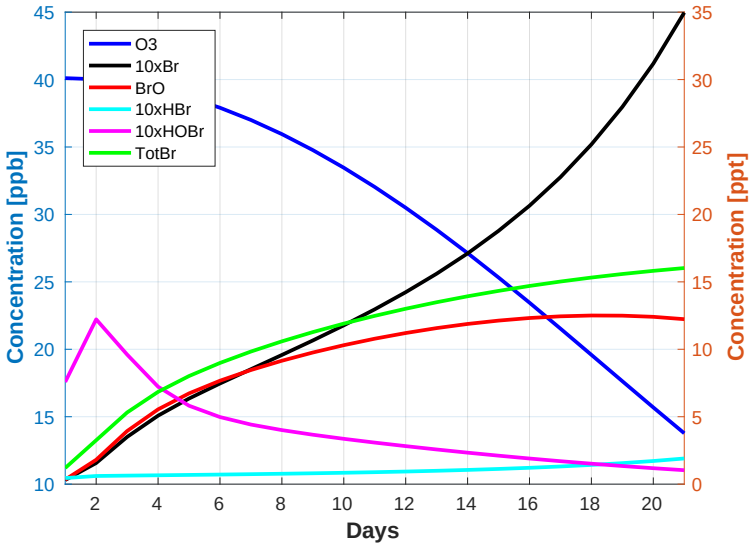

FIGURE 4.5: BoxJJA: Daily averages for O_3, $10 \times$ Br, BrO, $10 \times$ HBr, $10 \times$ HOBr and the total bromine molecules over the course of 21 days.

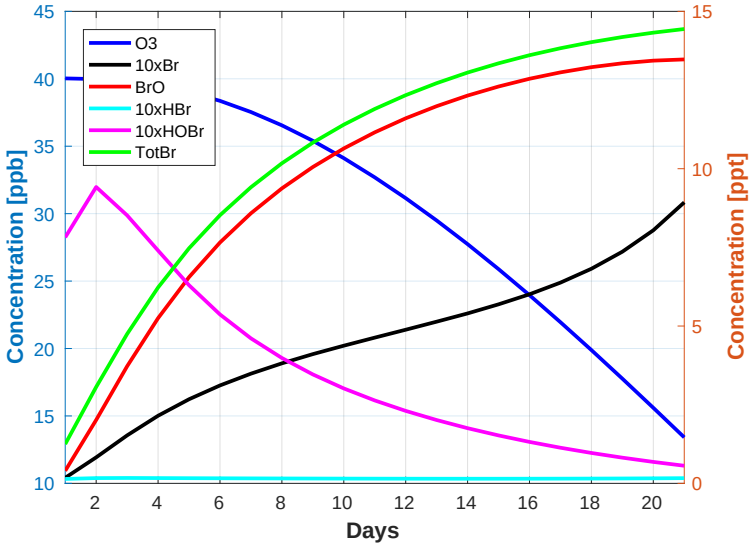

FIGURE 4.6: BoxSON: Daily averages for O_3, $10 \times$ Br, BrO, $10 \times$ HBr, $10 \times$ HOBr and the total bromine molecules over the course of 21 days.

4.1.4 Moving the Box

The grid box is now moved to $45.0°$N and to the Equator. In Figure 4.8 Br, HBr and BrO are all rising, so the ozone is not depleted as much as before. The ozone levels drop with 18 ppb over the 21 days. The same occurs in

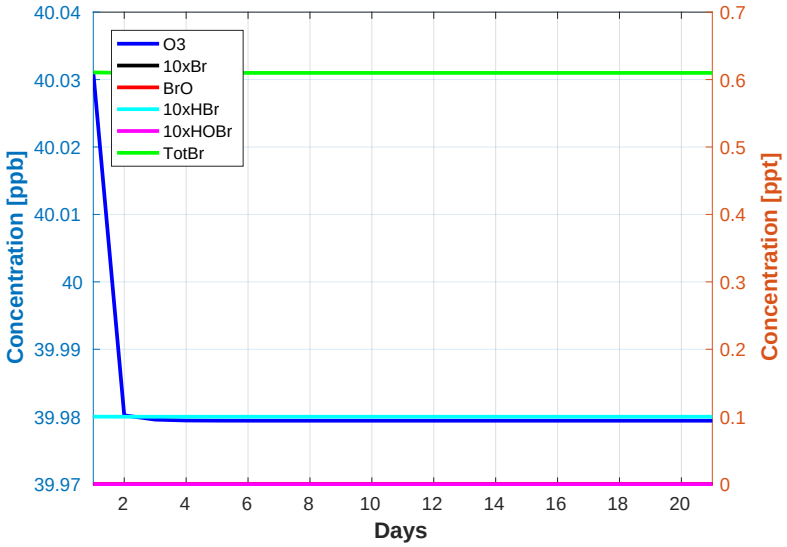

FIGURE 4.7: BoxDFJ: Daily averages for O_3, $10 \times$ Br, BrO, $10 \times$ HBr, $10 \times$ HOBr and the total bromine molecules over the course of 21 days.

Figure 4.9. The closer the box moves to Equator, the less efficient is the depletion of ozone. At Equator, the ozone drops by 13.5 ppb.

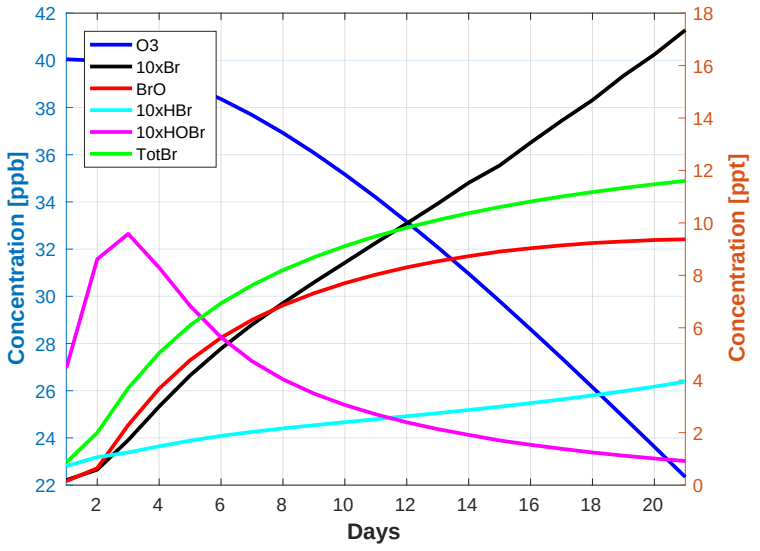

FIGURE 4.8: BoxLat45: Daily averages for O_3, $10 \times$ Br, BrO, $10 \times$ HBr, $10 \times$ HOBr and the total bromine molecules over the course of 21 days.

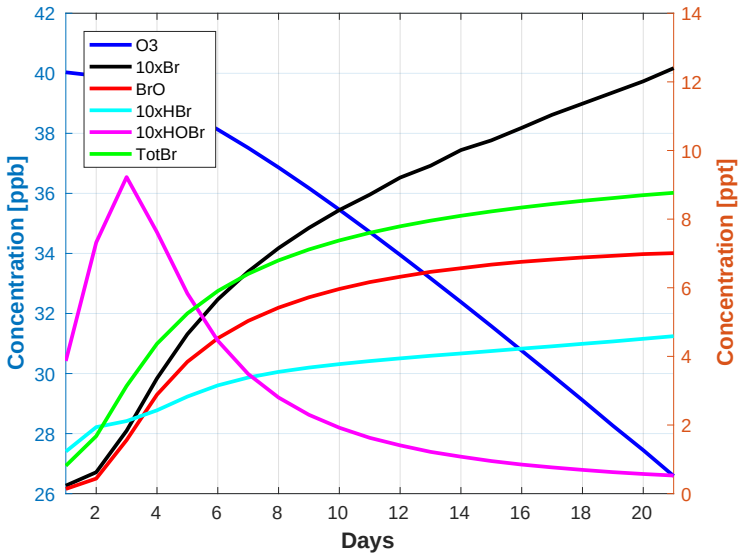

FIGURE 4.9: BoxLatEq: Daily averages for O_3, $10 \times Br$, BrO, $10 \times HBr$, $10 \times HOBr$ and the total bromine molecules over the course of 21 days.

4.1.5 Different Surface Conditions

As explained in Section 2.1.3, frost flowers increase the available surface area on which reactions can take place, and therefore increases the sources of Br_2 and BrCl, leading to the bromine explosion. Since it is already assumed that there is an occurence of frost flowers, β is tested for a flat surface, at unity, and for a potential surface with a lack of snow or ice, for instance an area with rocks, or open water, at 0.8.

As expected, the depletion of ozone goes down when β is lowered. Figure 4.10 shows a ozone drop of 7 ppb, against 21 ppb with β at 1.4 in the control experiment. The shape of HOBr is almost the same as in the control experiment, with a slightly shaper decrease in the first three days. However, it is shifted slightly upwards, suggesting a larger presence of HOBr in the air due to lack of interaction with snow and ice particles on the ground.

Figure 4.11 shows a drop in ozone of around 11 ppb. Again there is a slight shift of the HOBr curve, not as pronounced as in Figure 4.10, but nonetheless present. There is a larger rise in BrO then in BoxBeta0.8, but less than in the control experiment.

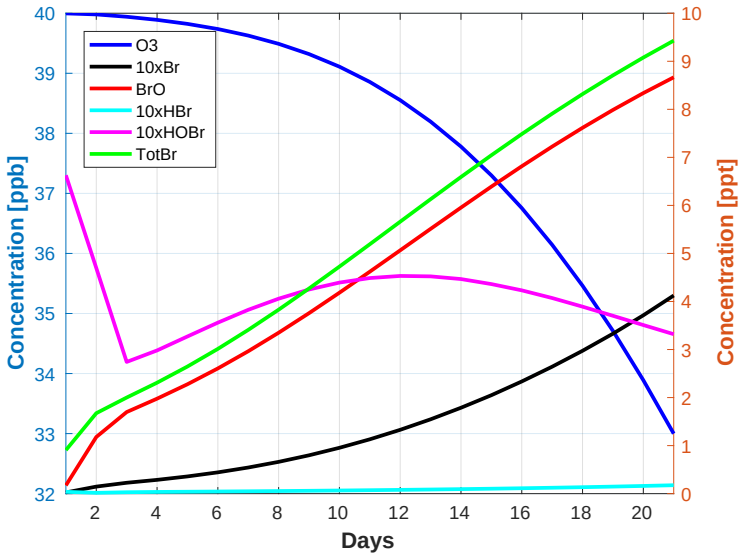

FIGURE 4.10: BoxBeta0.8: Daily averages for O_3, $10 \times Br$, BrO, $10 \times HBr$, $10 \times HOBr$ and the total bromine molecules over the course of 21 days.

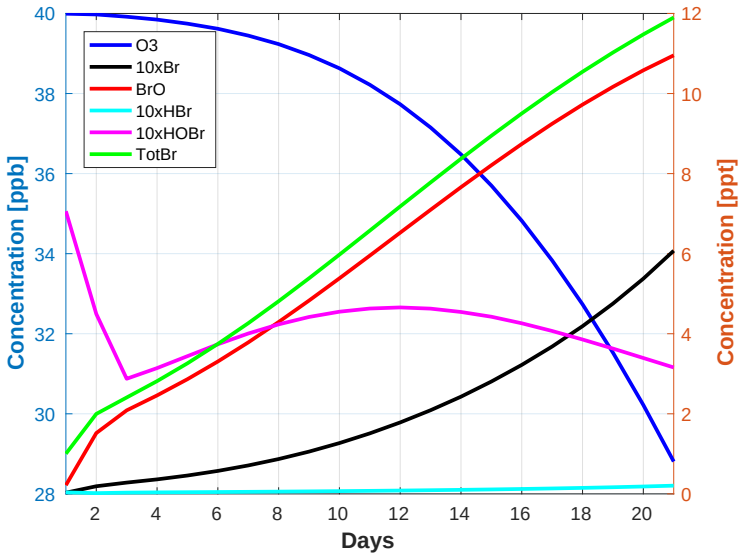

FIGURE 4.11: BoxBeta1.0: Daily averages for O_3, $10 \times Br$, BrO, $10 \times HBr$, $10 \times HOBr$ and the total bromine molecules over the course of 21 days.

4.1.6 Changing the ratio between R3 and R14

The ratio between R3 and R14 varies between 0.8 and 1.4. This affects the effectiveness of the bromine explosion by shifting between favoring R3 or R14. The experiments are run with 60% going to R3 and 40% to R14, Box,

and another one with 70% to R3 and 30% to R14. The shift is always done to favor R3 the most, since the aim is to get a bromine explosion.

The Figures shows drastic change in the ozone levels, and in Figure 4.13 the levels almost reach zero. This is what has been observed with measurements (Barrie et al., 1988, Martinez et al., 1999). The total bromine is mostly BrO, until the very last, where Br takes over, since the amount of ozone is very little, the reaction R5 is not longer favoured. This happens in Figure 4.12 as well, but to a smaller degree.

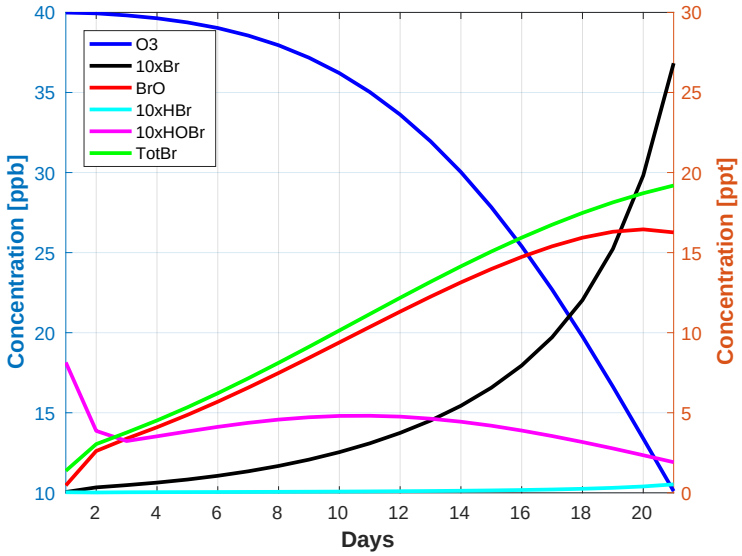

FIGURE 4.12: BoxRatio6040: Daily averages for O_3, $10 \times$ Br, BrO, $10 \times$ HBr, $10 \times$ HOBr and the total bromine molecules over the course of 21 days.

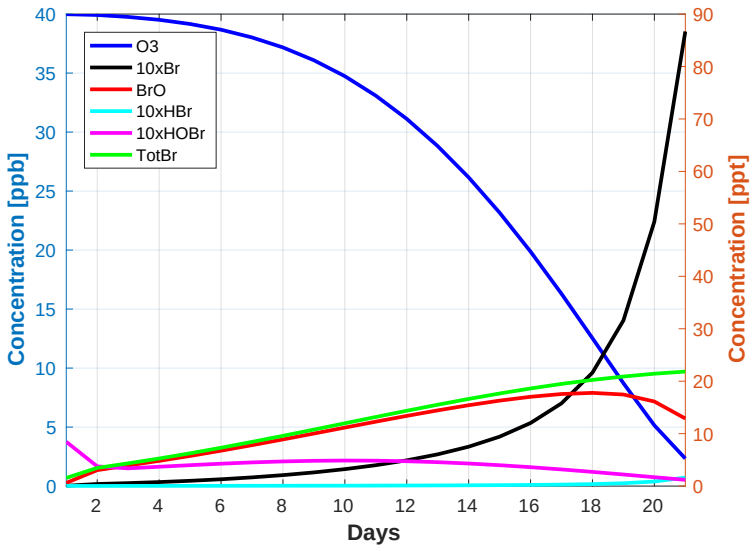

FIGURE 4.13: BoxRatio7030: Daily averages for O_3, $10 \times Br$, BrO, $10 \times HBr$, $10 \times HOBr$ and the total bromine molecules over the course of 21 days.

Chapter 5

Discussion And Conclusion

5.1 Changing the Height of the Boundary Layer (BL)

Since the most dominant steps in fuelling the bromine explosion is the release of Br_2 from the snowpack and the deposition of HOBr (Cao et al., 2016), adding extra height to the BL slows the depletion down. It gives time for the wind to transport the molecules away from the site, turbulent mixing to bring in fresh air and prevents the HOBr from settling onto the snow. And it takes longer time for the HOBr to reach the ground, it won't get to the stage of an explosion.

It is thought that the wind can contribute to ozone depletion by transporting fragments of frost flowers, blowing the snow, or through wind pumping, pressure differences which causes snow/ice to be lifted (Cao et al., 2016). However, it is the chemistry in the snowpack which mostly determines the Ozone Depletion Event (ODE) (Cao et al., 2016).

In this experiment, the same concentration of molecules are spead over a larger area, so the likelyhood of them colliding with each other and react is lower.

Following this experiment, L_{mix} is set to 200 meters in the Chemical Transport Model 3 (CTM3) model. The thickness of the BL is a key element in order to get a successful ODE, so it is essential that the meteorological data and the CTM3 is able to handle thin layers, which may not be the case.

5.2 Seasonal Variation

The ODE depends on the sun, so when there is no sun, there will be no depletion either. However, the ODE is a spring phenomenon, so it shouldn't be so much depletion over the summer. The ozone should start to regenerate faster and the snow conditions change, altering the sources of Br_2 and BrCl. Also, since the sources at the start of the run is the same as in spring and fall, the depletion will be efficient. In real life, the ozone formation

should become more efficient as the summer starts, as there is more sunlight available, which will limit the depletion.

The box model is a very simple model though, and these experiments are probably unrealistics in that the sources of Br^- and Cl^- are umlimited even under summer conditions. The snow/ice cover changes drastically during the summer and fall, meaning that there will be less bromine and chlorine available. Changing the β over the course of the seasons would help model this effect.

In the CTM3 the sources will be changing over the season, so it is expected that this issue does not arise during the runs.

5.3 Moving the Box

The reason for doing this is to see the efficiency at different latitudes. As the ODE is a phenomenon at the poles, it was expected that the depletion should drop.

One reason could be that as the box gets closer to Equator, the days becomes shorter, which limits the photolysis.

Another reason could be that the parameterization used in the box model for modelling the heterogenous reations R3 and R14 are tuned in for conditions with sea ice, making it unrealistic for lower latitudes.

The drop is a good thing though, and it is not expected to occur outside the Arctic in the CTM3 model.

5.3.1 Changing the Ground Conditions

The results from the experiment show that not including the frost flowers will limit the ODE. Cao et al., 2016 finds that the ODE happens in the very top layer of the snowpack, and having a smaller surface will limit the Br_2 and BrCl released from the snow. The CTM3 is run with β at 1.4.

5.3.2 Changing the ratio between R3 and R14

From the results, it is known that the ratio with 70 % towards R3 and 30 % towards R14 creates a complete ODE. The ratio $\frac{k_{R3}}{k_{R14}}$ is much higher than it should be though, so some consideration is taken before it is used in the CTM3 model.

Manipulating the ratio in this way gives the final push in order to get a full ODE, however, it would be unrealistic, and computing the chemistry more realistic is more important than getting a complete ODE. So in the CTM3, the ratio is still set to fifty-fifty. It could be interesting to look at this effect in the CTM3 though.

5.3.3 Conclusion

From the different runs it is found that changing the height of the BL drastically lowers the ozone depletion and the seasonal variation cannot really be represented with such a simple model. Moving the box to lower latitudes will have a negative effect on the ozone depletion, same if the ground conditions are changed to include less snow/ice. Changing the ratio between R3 and R14 gives a more unrealitic representation, though the ODE is shown more clearly.

Investigating with the box model is a good way of testing different theories and see them in action. The results can then be applied to the more complex CTM3.

Chapter 6

Model: CTM3

This chapter describes the Chemical Transport Model 3 (CTM3) used in this study (Section 6.1), the setup, modifications and input data (Section 3.2).

6.1 The CTM3

The CTM3 model is a tree dimensional global model developed by the University of Oslo and then expanded further by Center for International Climate and Enviromental Research - Oslo (CICERO). It is a so-called "offline" model, it uses meteorological forecast data from European Centre for Medium - Range Weather Forecasts (ECMWF) openIntegrated Forecast System (IFS) model at 3 hour intervals (Søvde, 2016). It can be run in two modes, one with both the stratosphere and the troposphere chemistry running, and one with only the troposphere chemistry. When run in troposphere mode only, the modelling is done up to a certain altitude, determined by the LMTROP variable. The LMTROP is the uppermost level, and is also seen as the tropopause. The height of the tropopause is based on the Potential Vorticity (PV) and the potential temperature.

The model runs with 60 vertical layers, with the topmost layer, with a thickness of 10 km, is centered at 0.11 hPa, or around 60 km (Søvde et al., 2012). A Gaussian grid is applied for the horizontal resolution, and the standard used in the CTM3 is T42, indicating a truncation number of 42, or a grid of $2.8°\times\ 2.8°$. However, the model can be run with the original resolution of the IFS, which is T319, $\ 0.5°\times\ 0.5°$.

Following (Prather, 1986) and later (Prather et al., 2008), the CTM3 uses Second Order Moment (SOM)s scheme for calculating the transport by advection. The first order moments contain information about the slope between two grid boxes, while the second order moments carry information about the curvature. This information is transported together with the mean grid box values.

The meridional and zonal winds are meteorological field updated at 3-hour instantous values, and are then used to calculate the vertical field.

In the CTM3 the washout for both aerosols and molecules is included, however, since the rain is prescribed for datasets, the model does not calculate Cloud Condensation Nuclei (CCN). For some easily soluble species, such as HNO_3, the sweepout can be calculated for large scale scavenging (Søvde, 2016). In convection scavenging, both ice and liquid is treated as rain, and when the liquid falls from one gridbox into a gridbox with dryer condition, it will experience evporation. However, whereas this is the case for liquid droplets, for ice droplets the process might be irreversible. There have been updates in the structure of the model (Søvde et al., 2012), which has made some differences with the amounts removed by convective percipitation.

Vertical transport by convection is calculated as a separate process, using mass fluxes from updrafts and downdrafts. The entrainment and detrainment are separated into two categories, the turbulent exchange through cloud edges, and organized exchanges.

The photodissociation is calculated online following Prather, 2012 using the fast - JX method. The values can be calculated every chemical time step, or once every step of the operator split, the duration of each process, default is 1 hour (Søvde, 2016). The sea salt production is calculated from the winds, and the flux is then used to calculate the flux of organic matter from the ocean.

6.2 Setup of the CTM3

The model were set up to run with the troposphere chemistry only, excluding the stratosphere, in order to shorten the running time, and changes in the stratosphere will have small effect on the Ozone Depletion Event (ODE) close to the surface. This also omit the emission of CH_3Br, see Section 6.4 for more detailed info regarding this. Other than that the model is run with the sulphur mode and the emission + deposition inside chemistry mode on. The rest, Black Carbon (BC)/organic carbon, seasalt, nitrate and mineral mode is turned off. That has been done in order to better isolate the ODE, and shorten the CPU-time.

Originally, the troposphere has 46 components included in the chemistry scheme, however, this number has now been changed to 62, 51 being transported.

The model runs start the 30th of April 2012, and run for 32 days. The reason this date was chosen is that in May 2012, there was on ODE in both Alert, Canada, and in Barrow, Alaska, USA, so the meteorological conditions should be more ideal

6.3 Modifications done in the CTM3

There has not been any chemistry regarding bromine and chlorine included in the tropospheric part of the CTM3, so there are some steps that must be completed in order to include them in the chemistry routine. First the chemical reactions chosen are included, explained in Section 6.3.1. Secondly the rates are addressed, described in Section 6.3.2. At the end the sources for halogens from the ocean are included, see Section 6.4.

After the scheme is implemented, results for specific locations are chosen in order to be able to compare with observations, see Section 6.4.1.

6.3.1 Implementing the halogen chemistry

Since the reactions introduced in the box model managed to represent the ODE well, the same reactions are now included in the CTM3:

$$\mathrm{HOBr} + h\nu \longrightarrow \mathrm{Br} + \mathrm{OH} \quad \text{(R1)}$$
$$\mathrm{HOBr} + \mathrm{HBr} \xrightarrow{mp} \mathrm{Br_2} + \mathrm{H_2O} \quad \text{(R2)}$$
$$\mathrm{HOBr} + \mathrm{H^+} + \mathrm{Br^-} \xrightarrow{snow} \mathrm{Br_2} + \mathrm{H_2O} \quad \text{(R3)}$$
$$\mathrm{Br_2} + h\nu \longrightarrow 2\mathrm{Br} \quad \text{(R4)}$$
$$\mathrm{Br} + \mathrm{O_3} \longrightarrow \mathrm{BrO} + \mathrm{O_2} \quad \text{(R5)}$$
$$\mathrm{BrO} + \mathrm{BrO} \longrightarrow 2\mathrm{Br} + \mathrm{O_2} \quad \text{(R6)}$$
$$\mathrm{BrO} + h\nu \longrightarrow \mathrm{Br} + \mathrm{O} \quad \text{(R7)}$$
$$\mathrm{BrO} + \mathrm{HO_2} \longrightarrow \mathrm{HOBr} + \mathrm{O_2} \quad \text{(R8)}$$
$$\mathrm{Br} + \mathrm{HO_2} \longrightarrow \mathrm{HBr} + \mathrm{O_2} \quad \text{(R9)}$$

$$\mathrm{BrO} + \mathrm{NO} \longrightarrow \mathrm{Br} + \mathrm{NO_2} \quad \text{(R10)}$$
$$\mathrm{BrO} + \mathrm{NO_2} + (\mathrm{M}) \longrightarrow \mathrm{BrONO_2} + (\mathrm{M}) \quad \text{(R11)}$$
$$\mathrm{BrONO_2} + \mathrm{H_2O} \xrightarrow{mp} \mathrm{HOBr} + \mathrm{HNO_3} \quad \text{(R12)}$$

$$\mathrm{HOBr} + \mathrm{HCl} \xrightarrow{mp} \mathrm{BrCl} + \mathrm{H_2O} \quad \text{(R13)}$$
$$\mathrm{HOBr} + \mathrm{H^+} + \mathrm{Cl^-} \xrightarrow{snow} \mathrm{BrCl} + \mathrm{H_2O} \quad \text{(R14)}$$
$$\mathrm{BrCl} + h\nu \longrightarrow \mathrm{Br} + \mathrm{Cl} \quad \text{(R15)}$$
$$\mathrm{Cl} + \mathrm{O_3} \longrightarrow \mathrm{ClO} + \mathrm{O_2} \quad \text{(R16)}$$
$$\mathrm{OH} + \mathrm{ClO} \longrightarrow \mathrm{Cl} + \mathrm{HO_2} \quad \text{(R17)}$$
$$\mathrm{OH} + \mathrm{ClO} \longrightarrow \mathrm{HCl} + \mathrm{O_2} \quad \text{(R18)}$$

Reactions (R1-R9) are reactions with bromine only, while reactions (R10-R12) are reactions with nitrogen, and (R13-R18) are chemical reactions with chlorine.

Unlike in the box model, these components are already included in the CTM3. However, the bromine and chlorine components are only included in the stratosphere, and with this turned off, they are no longer represented in the model. So they are now implemented into the troposphere, together with the reactions stated above. Nitrogen already has a well-developed scheme, so computing these requires little work. For the chlorine and bromine part, however, considerable modifications must be carried out.

6.3.2 Rates

Some of the reactions added to the troposphere part of the CTM3 are in the stratopshere part already, so there are rate constants already available. Therefore the rate constants will be slightly different compared to the ones in the box model. However not all the reactions are included in the statosphere part, in this case the rate constants from Cao et al., 2014 will be used. The rate constants are listed in table 6.1.

Reactions R2, R13 and R12 are implemented in a subroutine called `TCRATE_TP_IJ_TRP`. The implementation is done in the same way as in the box model, described in Section 3.2.4. The same parameters are also used, listed in table 3.6. The CTM3 already have a subroutine calculating the uptake coefficients. Though the representation is a bit different (Søvde, 2016), so in order to be consistant and to have better control over the process, the method from the box model is employed.

6.4 Sources of Halogens

Since the CTM3 is more complex and resembles nature better than the box model, sources of halogens from the sea are included. Since the model is not run with set starting values as in the box model, there won't be any halogens in the troposphere, which means that the reactions R3 and R14 won't release more halogens into the atmosphere.

The reactions are taken from (Parrella et al., 2012). Originally CH_3Br is included in the model as a source on the ten bottom layers (Søvde, 2016). This is in order to transport the component to the stratosphere and start the reactions there. There are no chemistry involved for this compound in the troposhere, other than photolysis. Since the CTM3 is run without the stratosphere, this is not included. Instead these sources are used:

$$CHBr_3 + OH \longrightarrow 3Br + \text{products} \quad \text{(R19)}$$

$$CH_2Br_2 + OH \longrightarrow 2Br + \text{products} \quad \text{(R20)}$$

$$CHBr_3 + h\nu \longrightarrow 3Br + \text{products} \quad \text{(R22)}$$

In order to save time, the the two components CH_2Br_2 and $CHBr_3$ are connected into one, named CH_3Br. The naming is done this way since the CH_3Br already exists, as stated above. Without the stratosphere, this array is not included, and can therefore be used. The photolysis of R22 is calculated using the CH_3Br array.

$$CH_3Br \begin{cases} CH_2Br_2 \\ CHBr_3 \end{cases}$$

Adding an extra component requires more comprehensive changes to the CTM3. Since the only purpose is to gain a source of bromine from the sea, combining them into one variable is more efficient.

In order to capture the emissions in a good way, scenario A from (Liang et al., 2010) is employed. The scenario describes latitude-bands with given emissions from the marine biosphere, with higher emission along the coasts, visualized in figure 6.1. The scheme does not include seasonal changes, however the model used did produce seasonal variations (Liang et al., 2010). Out of the three scenarios decribed in Liang et al., 2010, Scenario A is the only one that covers emissions further north/south of $50°$. This scheme also desplayed good estimates compared to the observed measured vertical profile and model simulations. A factor of $1.14 \times \frac{2}{3}$ is added to represent the CH_2Br_2

The values for each latitude-band is read from figure 6.1, and the mid-value is taken. This means that from 80°S to 50°S, the emissions are 0.05×10^{-13} $kgm^{-2}s^{-1}$ for the open ocean and 0.05×10^{-13} $kgm^{-2}s^{-1}$ for the coast.

6.4.1 Locations

In order to compare the results from the simulations to observations, three locations are chosen:

- Zeppelin, Svalbard, Norway (ZEP)
- Alert, Canada (ALT)
- Barrow, Alaska, USA (BAR)

These locations have long history of ODEs, and several studies have been conducted here, especially at Alert and Barrow (Barrie et al., 1988, Bottenheim et al., 1986, Martinez et al., 1999).

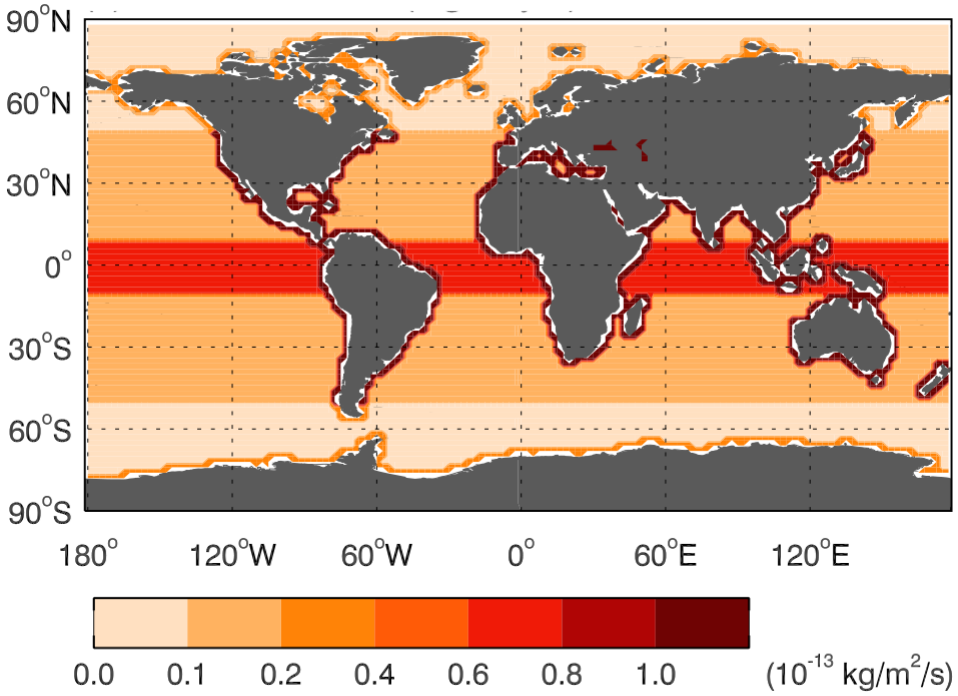

FIGURE 6.1: Global emission distribution of $CHBr_3$. Modified from (Liang et al., 2010).

TABLE 6.1: Expressions used for calculating the rate in the CTM3

Reaction No.	Rate Expression	Unit	Reference
R1	Expresssion from the CTM3		
R2	See table 3.6	-	(Cao et al., 2014)
R3	$\frac{V_d}{L_{mix}} \times \beta$	s^{-1}	(Cao et al., 2014)
R4	Expression from the CTM3		
R5	$1.7 \times 10^{-11} \exp(\frac{-800}{T})$	$cm^3\ molecules^{-1}\ s^{-1}$	(Sander et al., 2006)
R6	$2.4 \times 10^{-12} \exp(\frac{40}{T})$	$cm^3\ molecules^{-1}\ s^{-1}$	(Sander et al., 2006)
R7	Expression from the CTM3		
R8	$4.5 \times 10^{-12} \exp(\frac{460}{T})$	$cm^3\ molecules^{-1}\ s^{-1}$	(Sander et al., 2006)
R9	$4.8 \times 10^{-12} \exp(\frac{-310}{T})$	$cm^3\ molecules^{-1}\ s^{-1}$	(Sander et al., 2006)
R10	$8.8 \times 10^{-12} \exp(\frac{260}{T})$	$cm^3\ molecules^{-1}\ s^{-1}$	(Sander et al., 2006)
R11	3.89×10^{-12}	$cm^3\ molecules^{-1}\ s^{-1}$	(Sander et al., 2006)
R12	See table 3.6	-	(Cao et al., 2014)
R13	See table 3.6	-	(Cao et al., 2014)
R14	$\frac{V_d}{L_{mix}} \times \beta$	s^{-1}	(Cao et al., 2014)
R15	Expresssion from the CTM3		
R16	$2.3 \times 10^{-11} \exp(\frac{-200}{T})$	$cm^3\ molecules^{-1}\ s^{-1}$	(Sander et al., 2006)
R17	$7.4 \times 10^{-12} \exp(\frac{270}{T})$	$cm^3\ molecules^{-1}\ s^{-1}$	(Sander et al., 2006)
R18	$6.0 \times 10^{-13} \exp(\frac{230}{T})$	$cm^3\ molecules^{-1}\ s^{-1}$	(Sander et al., 2006)

TABLE 6.2: Expressions used for calculating the rate for halogen sources in the CTM3

Reaction No.	Rate Expression	Unit	Reference
R19	$1.35 \times 10^{-12} \times \exp(\frac{-600}{T})$	$cm^{-3}\ molecules^{-1}\ s^{-1}$	(Parrella et al., 2012)
R20	$2.00 \times 10^{-12} \times \exp(\frac{-840}{T})$	$cm^{-3}\ molecules^{-1}\ s^{-1}$	(Parrella et al., 2012)
R22	1.1×10^{-6}	s^{-1}	(Parrella et al., 2012)

Chapter 7

Result: CTM3

7.1 Results

The Chemical Transport Model 3 (CTM3) runs did not go as planned. There are some errors in the programmed that could not be fixed in time, so the plots shown is not the expected results.

All the plots shown are from Alert, Canada, starting 30th of April 2012.

The errors could just attributed to the fact that there is a well-mixed Boundary Layer (BL), as well as the resolution being to coarse. However, unlike what is said in the setup for the CTM3, Section 6.2, the runs do not last 32 days. After 14 days, CH3Brx1 blows up, and for CH3Brx1000, this happens after 10 days.

Figure 7.1 shows the ozone levels for the control run, O_3 Original, with only the sulphur mode and the emission and deposition mode on. It also shows the ozone levels for CH3Brx1 run. The levels stay the same until day 10, when the CH3Brx1 starts to grow and blow up.

Figure 7.2 shows the ozone levels of the original run, together with CH3Brx1 and CH3Brx1000, over the course of 10 days. It runs for 10 days since the values in the CH3Brx1000 blows up after this.

CH3brx1 and CH3Brx1000 are almost the same all the time, with a small exception of the last two days, where the CH3Brx1 starts to rise. The restof the climb is shown in Figure 7.1.

Figure 7.3 display the CH3Brx1 run, with Bry and HOBr on the left axis, in ppm, and HCl, Cly, $CHBr3$, ClO, HBr and BrCl on the right axis, in ppt. THe run lasts 14 days. Bry and HOBr rise to extremly high values, around 4000ppm, which is very unrealistic and clearly wrong.

Figure 7.3 display the run CH3Brx1000, with Bry and HOBr on the left axis, in ppb, and HCl, Cly, $CHBr3$, ClO, HBr and BrCl on the right axis, in ppt. The run goes on for 10 days. Again the values rise to the extreme, but not as extreme as CH3Brx1.

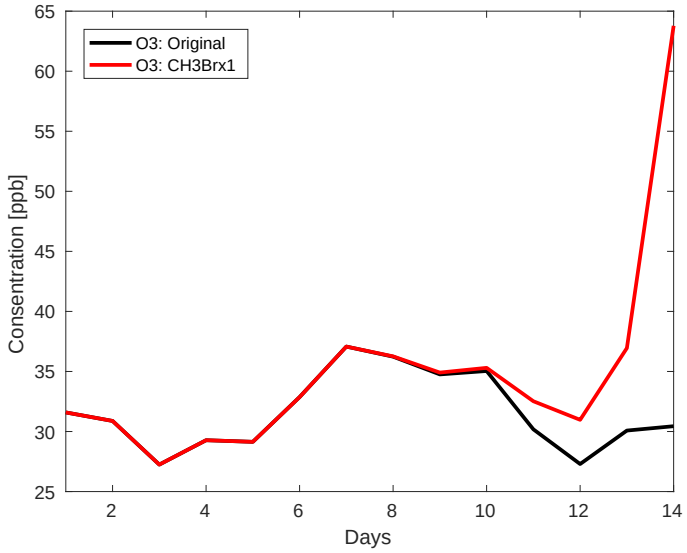

FIGURE 7.1: O3: Original is the original model as explained in Section (REF), while the O3: CH3Brx1 is the modified model run with emissions from CH_3Br, with concentration shown in ppb. The plot shows the average daily values over 14 days, starting 30th of April 2012, at Alert, Canada

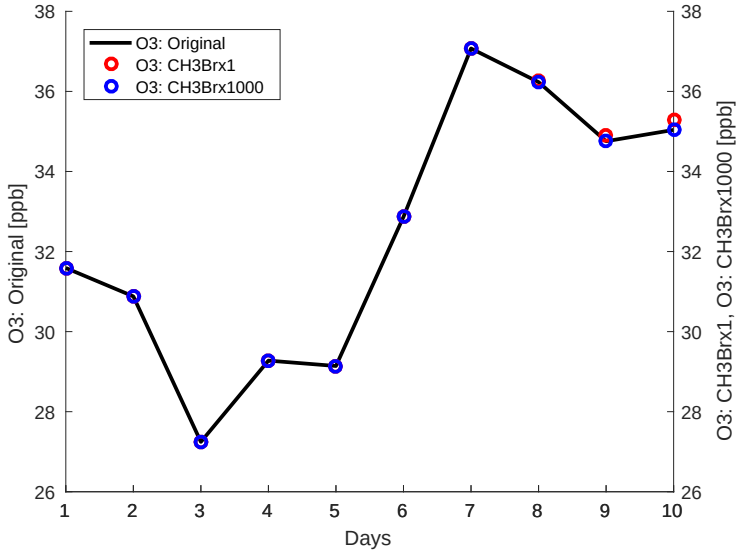

FIGURE 7.2: Plot showing the averaged daily values of O_3 for the original model, with CHBr3 $\times$ 1, and with CHBr3 $\times$ 1000. Consentration is shown in ppb. The location is Alert, Canada, starting the 30th of April, 2012

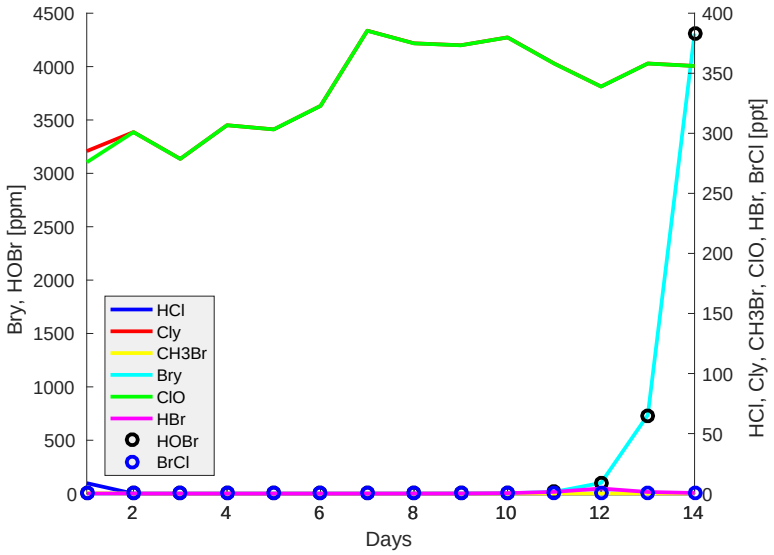

FIGURE 7.3: Plots shows the average daily values for all the species from the model run CH3Brx1, except O_3. Bry and HOBr are shown on the left axis, in ppm, and while HCl, Cly, $CHBr3$, ClO, HBr and BrCl are shown on the axes on the right hand side, in ppt. The plot is from Alert, Canada, starting 30th of April 2012

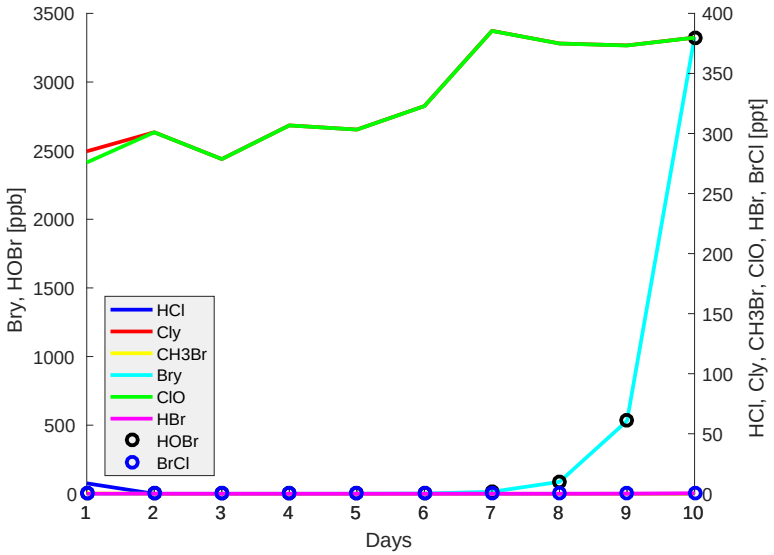

FIGURE 7.4: Plots shows all the elements from the model run CH3Brx1000, except O_3. Bry and HOBr are shown on the left axis, in ppb, and while HCl, Cly, $CHBr3$, ClO, HBr and BrCl are shown on the axes on the right hand side, in ppt.

Chapter 8

Discussion and Conclusion

8.1 Discussion

The results from the CTM3 model clearly illustrates an error or many errors in the program, however, it could not be fixed in time for the completion of the thesis.

Regardless whether the model worked or not, there are some issues which should be mentioned.

Rate constant k for R11 exists in the Chemical Transport Model 3 (CTM3), but is only included in the stratosphere. This has not been used. Instead, the expression is taken from Cao et al., 2014. As the stratosphere chemistry is turned of, this rate constant will not be active, unless included in the troposphere. Instead, it was chosen to include the expression from Cao et al., 2014, because it shown in the box model that this is a good expression.

From Chapter 2, α_{eff} is constant, even though it depends in the size of the box. Ideally, this should be changed so that α_{eff} changes as the volume of the grid box varies.

In the sources of halogens, there is a simplification done with CH_3Br, which in reality contains both CH_2Br_2 and $CHBr_3$. The factor ($1.14 \times (\frac{2}{3}$) is included in order to compansate the lack of chemical components in the model. Adding another components to the chemistry scheme is not hard, however, adding a new photolysis reaction is much worse, hence the simplification. If might be in idea for the future to look into this issue.

The sources of halogens are only the ones from the ocean, which are the dominate ones. There are no anthropogentic sources. It could be interesting to see the effect of adding anthropogenic sources to the model.

A major issue with the model is the resolution. The results are run with a resolution of 2.8 °$\times$ 2.8 °, a very coarse resolution. Especially considering the fact that only single-spot locations are chosen. Since the results from Chapter 7 displays the average from four gridboxes around the chosen location, the ozone and the halogens will drop when averaged. This can be

prevented to a certain degree by chosing one out of the four boxes and stick with it.

8.1.1 Future Aspects

Getting the model to run properly is on high priority. It would also be good to investigate the issues mentioned in the previous Section. Running the model with a smaller resolution should also be done, in order to resolve the local changes much better.

With the model being fixed, the step in the plan could start, calculating the change in Radiative Forcing (RF) due to the presence of halogen. And from there calculate the temperature change due to halogens.

8.1.2 Conclusion

Even though the results from the CTM3 did not turn out as expected, it was worth trying. And from the results from the box model, it is seen that the reactions give the desired effect and therefore can be used.

Appendix A

Initializing the Box Model

TABLE A.1: Initial mixng ratios of tracers in the box model.

Species	Mixing ratio
O_3	40.0 ppb
OH	0.4 ppb
HO_2	0.4 ppb
H_2H_2	1.0 ppt
$RO2$	0.4 ppb
NO	5.0 ppt
NO_2	10.0 ppt
HNO_3	1.0 ppt
N_2O_5	1.0 ppt
CO	132.0 ppb
CH_4	1.9 ppm
CH_3O_2H	1.0 ppt
$HCHO$	100.0 ppt
O^3P	0.4 ppb
NO_3	0.4 ppb
HC	1.0 ppb
Br_2	0.3 ppt
HBr	0.1 ppt
HCl	0.01 ppt
$BrONO_2$	0.0
HBr	0.0
Br	0.0
BrO	0.0
$BrCl$	0.0
Cl	0.0
ClO	0.0

A.1 Experiments with the Box Model

The Appendix shows the plots from the box model. The plots visualize the Ozone Depletion Event (ODE) over the course of 21 days. All the plots show the ozone values on the left hand side, in ppb, while the right hand side shows the halogens, in ppt.

A.1.1 Changing the Height of the Boundary Layer (BL)

Figure A.1 shows the chlorine and ozone when the BL is changed to 500m. There is little change to see, but as in previous plots, the ClO is the dominant molecule.

Figure A.2 is the same scenario as above, but now the height of the BL is 1000m.

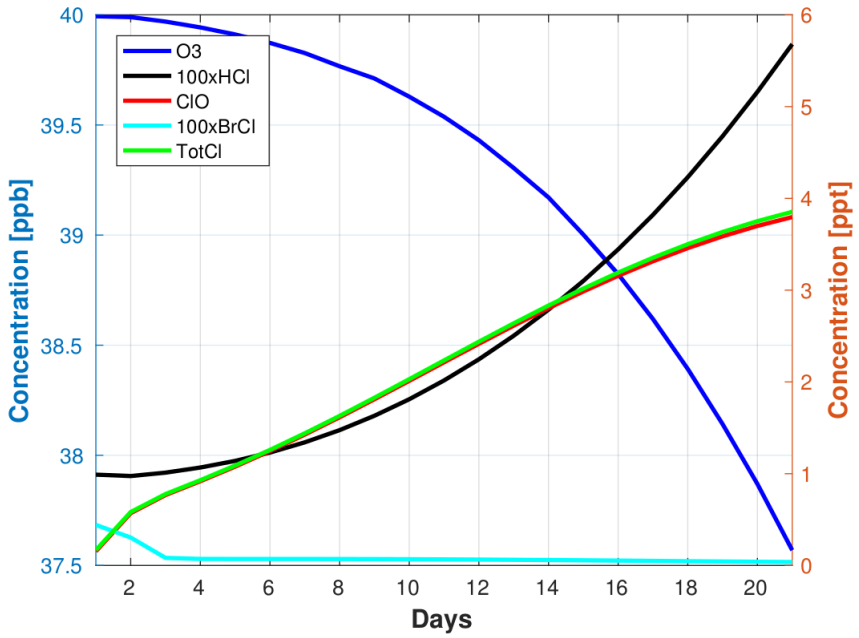

FIGURE A.1: BoxBL500: Daily averages for O_3, $100 \times$ HCl, ClO, $100 \times$ BrCl and the total chlorine molecules.

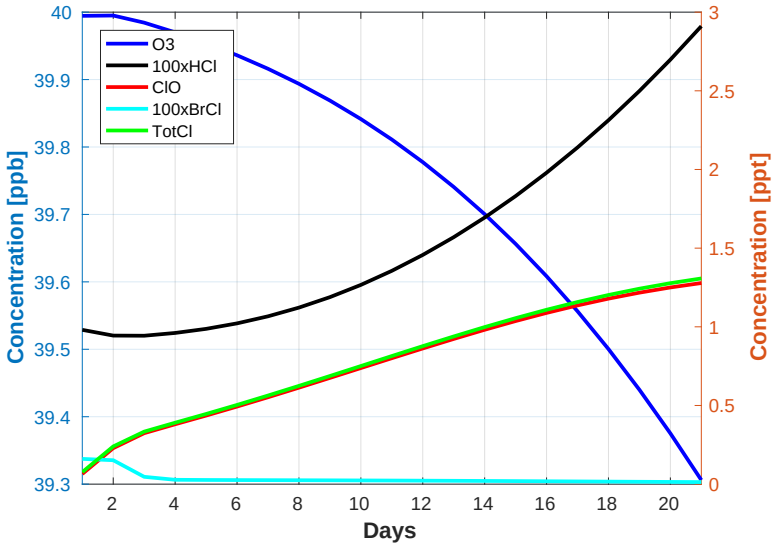

FIGURE A.2: BoxBL1000: Daily averages for O_3, $10 \times$ Br, BrO, $10 \times$ HBr, $10 \times$ HOBr and the total bromine molecules over the course of 21 days.

A.1.2 Seasonal Variation

The season is changed to summer, fall and winter. When the sun if gone, there is no depletion.

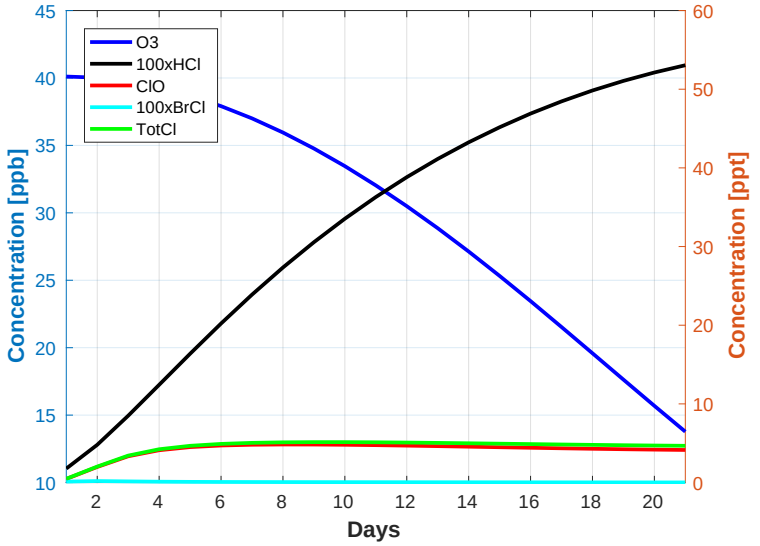

FIGURE A.3: BoxJJA: Daily averages for O_3, $100 \times$ HCl, ClO, $100 \times$ BrCl and the total chlorine molecules over the course of 21 days.

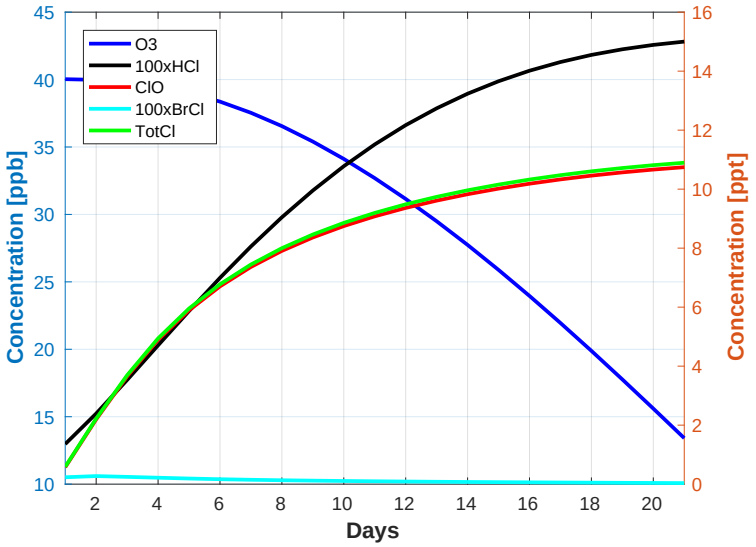

FIGURE A.4: BoxSON: Daily averages for O_3, $100 \times HCl$, ClO, $100 \times BrCl$ and the total chlorine molecules over the course of 21 days.

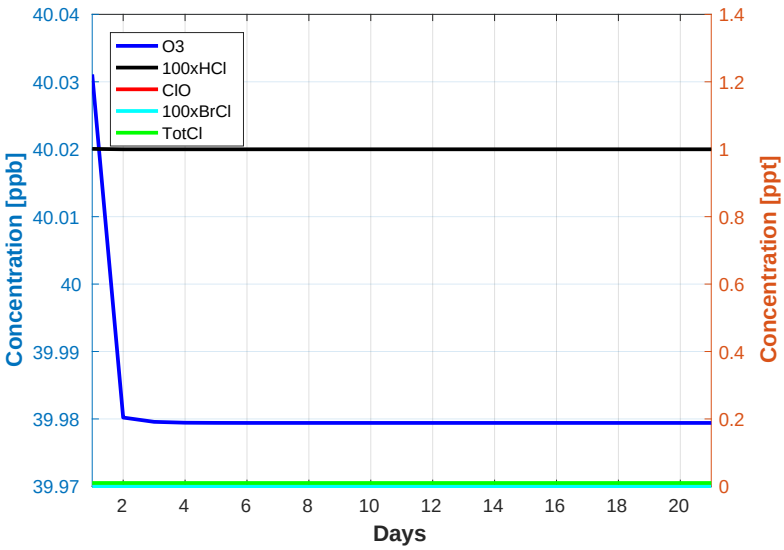

FIGURE A.5: BoxDFJ: Daily averages for O_3, $100 \times HCl$, ClO, $100 \times BrCl$ and the total chlorine molecules over the course of 21 days.

A.1.3 Moving the Box

The box is moved to 45 °N and to the Equator.

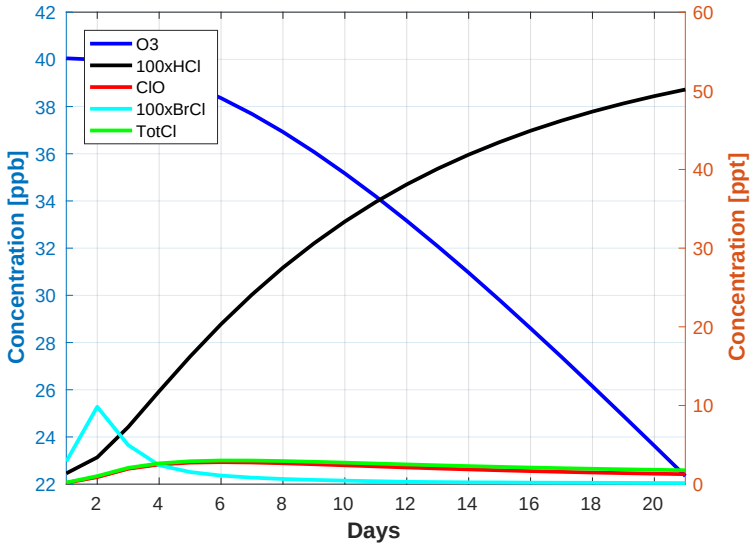

FIGURE A.6: BoxLat45: Daily averages for O_3, $100 \times HCl$, ClO, $100 \times BrCl$ and the total chlorine molecules over the course of 21 days.

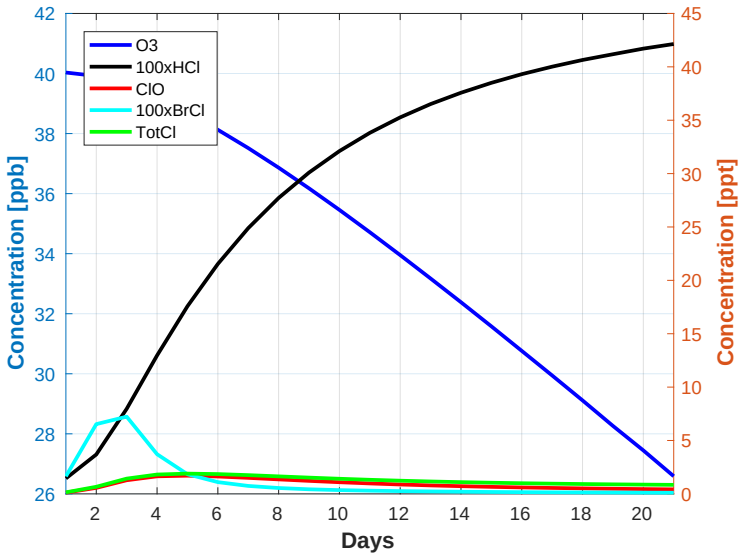

FIGURE A.7: BoxLatEq: Daily averages for O_3, $100 \times HCl$, ClO, $100 \times BrCl$ and the total chlorine molecules over the course of 21 days.

A.1.4 Changing the Ground Conditions

β is now changed to 0.8, Figure A.8 and 1.0, Figure A.9

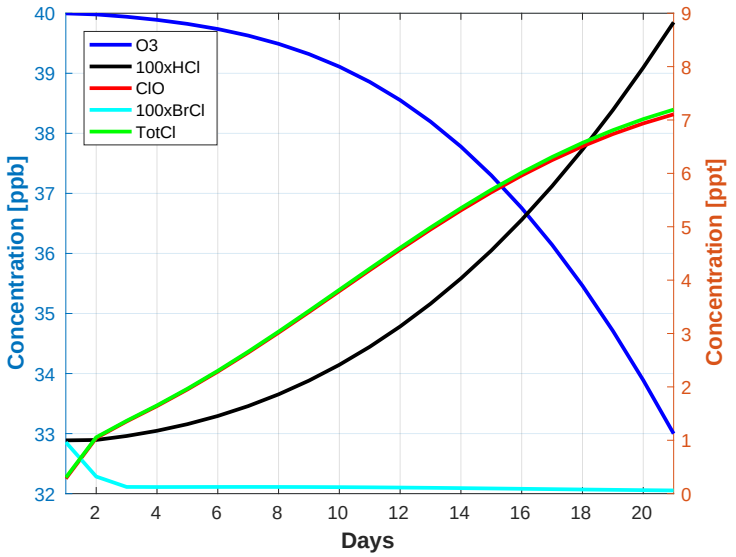

FIGURE A.8: BoxBeta0.8: Daily averages for O_3, $100 \times HCl$, ClO, $100 \times BrCl$ and the total chlorine molecules over the course of 21 days.

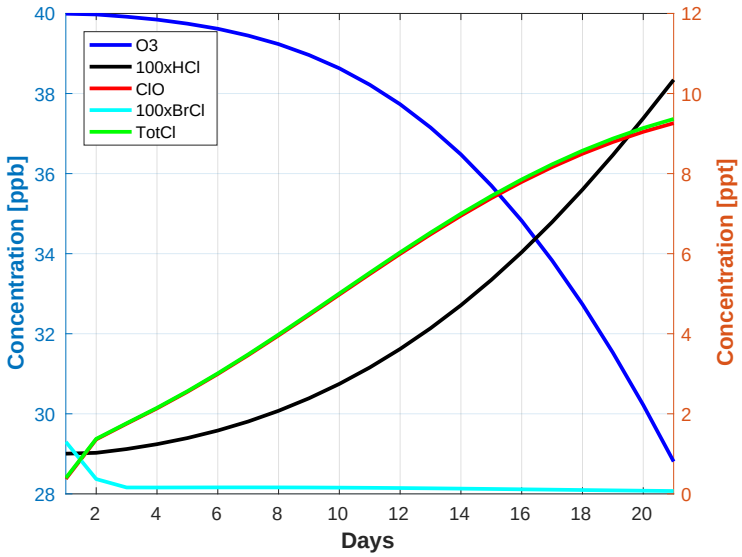

FIGURE A.9: BoxBeta1.4: Daily averages for O_3, $100 \times HCl$, ClO, $100 \times BrCl$ and the total chlorine molecules over the course of 21 days.

A.1.5 Changing the Ratio of R3 and R14

The ratio between R3 and R14 is changed to 60 % R3 and 40 % R3 and 70 % R3 and 30 % R14

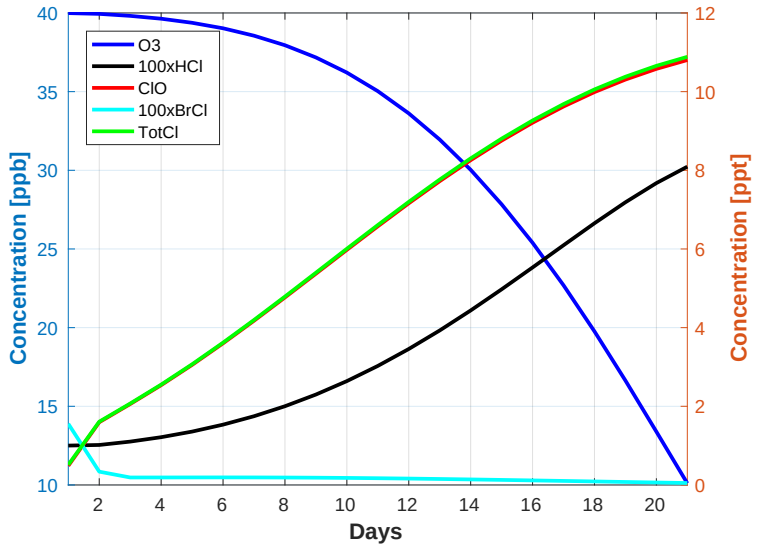

FIGURE A.10: BoxRatio0604: Daily averages for O_3, $100 \times HCl$, ClO, $100 \times BrCl$ and the total chlorine molecules over the course of 21 days.

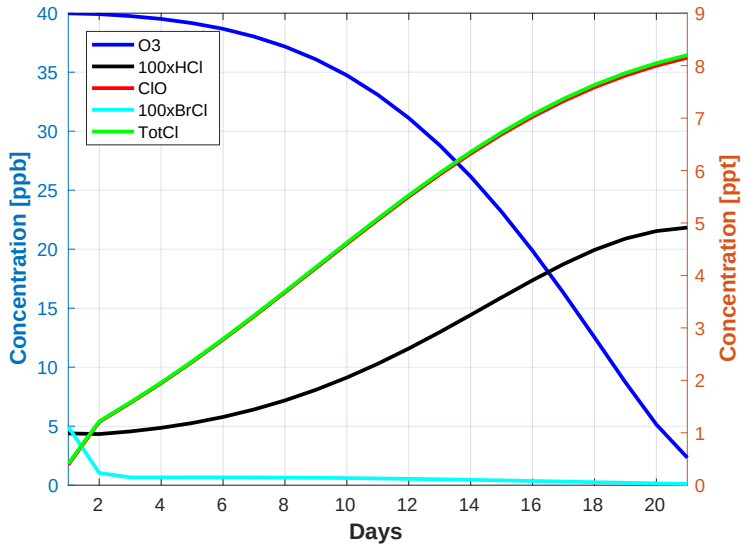

FIGURE A.11: BoxRatio0703: Daily averages for O_3, $100 \times HCl$, ClO, $100 \times BrCl$ and the total chlorine molecules over the course of 21 days.

Bibliography

Aardenne, JA van et al. (2001). "A 1× 1 resolution data set of historical anthropogenic trace gas emissions for the period 1890–1990". In: *Global Biogeochemical Cycles* 15.4, pp. 909–928. DOI: 10.1029/2000GB001265.

Ainsworth, Elizabeth A (2008). "Rice production in a changing climate: a meta-analysis of responses to elevated carbon dioxide and elevated ozone concentration". In: *Global Change Biology* 14.7, pp. 1642–1650.

Atkinson, R et al. (2010). "Evaluated kinetic and photochemical data for atmospheric chemistry". In: *Atmos. Chem. Phys.*

Barrie, LA et al. (1988). "Ozone destruction and photochemical reactions at polar sunrise in the lower Arctic atmosphere". In: *Nature* 334.6178, pp. 138–141. DOI: 10.1038/334138a0.

Beare, Robert J et al. (2006). "An intercomparison of large-eddy simulations of the stable boundary layer". In: *Boundary-Layer Meteorology* 118.2, pp. 247–272. DOI: 10.1007/s10546-004-2820-6.

Berntsen, Terje K et al. (1997). "Effects of anthropogenic emissions on tropospheric ozone and its radiative forcing". In: *Journal of Geophysical Research: Atmospheres* 102.D23, pp. 28101–28126. DOI: 10.1029/97JD02226.

Bottenheim, Jan et al. (1986). "Measurements of NOy species and O3 at 82 N latitude". In: *Geophysical Research Letters* 13.2, pp. 113–116. DOI: 10.1029/GL013i002p00113.

Bowman, Kevin W et al. (2013). "Evaluation of ACCMIP outgoing longwave radiation from tropospheric ozone using TES satellite observations". In: *Atmospheric Chemistry and Physics* 13.8, pp. 4057–4072. DOI: 10.5194/acp-13-4057-2013.

Cao, L et al. (2014). "Numerical analysis of the chemical kinetic mechanisms of ozone depletion and halogen release in the polar troposphere". In: *Atmos. Chem. Phys* 14.7, p. 377.

Cao, L et al. (2016). "Numerical Analysis of the Role of Snowpack in the Ozone Depletion Events during the Arctic Spring". In: *Atmos. Chem. Phys. Discuss., http://dx. doi. org/10.5194/acp-2016-553, in review*.

Crowley, JN et al. (2010). "Evaluated kinetic and photochemical data for atmospheric chemistry: Volume V–heterogeneous reactions on solid substrates". In: *Atmospheric Chemistry and Physics* 10.18, pp. 9059–9223. DOI: 10.5194/acp-10-9059-2010.

Daniel, JS et al. (2010). "Options to accelerate ozone recovery: ozone and climate benefits". In: *Atmospheric Chemistry and Physics* 10.16, pp. 7697–7707. DOI: 10.5194/acp-10-7697-2010.

Debaje, SB (2014). "Estimated crop yield losses due to surface ozone exposure and economic damage in India". In: *Environmental Science and Pollution Research* 21.12, pp. 7329–7338.

Flanner, Mark G (2013). "Arctic climate sensitivity to local black carbon". In: *Journal of Geophysical Research: Atmospheres* 118.4, pp. 1840–1851. DOI: 10.1002/jgrd.50176.

Foster, Krishna L et al. (2001). "The role of Br2 and BrCl in surface ozone destruction at polar sunrise". In: *Science* 291.5503, pp. 471–474. DOI: 10.1126/science.291.5503.471.

from, Retrieved March 2017 (2017). *Choose an ODE Solver (R2017a)*. The MathWorks, Inc.

Gillespie, Colin et al. (2015). "Exposure to environmentally-relevant levels of ozone negatively influence pollen and fruit development". In: *Environmental Pollution* 206, pp. 494–501.

Guicherit, Robert et al. (2000). "Tropospheric ozone trends". In: *Chemosphere-Global Change Science* 2.2, pp. 167–183.

Hanson, David R et al. (1994). "Heterogeneous reactions in sulfuric acid aerosols: A framework for model calculations". In: *Journal of Geophysical Research: Atmospheres* 99.D2, pp. 3615–3629. DOI: 10.1029/93JD02932.

Hartmann, Dennis L (1994). *Global Physical Climatology, volume 56 of International Geophysics Series*.

Huff, Amy K et al. (2000). "Gas-Phase Br2 Production in Heterogeneous Reactions of Cl2, HOCl, and BrCl with Halide- Ice Surfaces". In: *The Journal of Physical Chemistry A* 104.31, pp. 7284–7293. DOI: 10.1021/jp001155w.

— (2002). "Kinetics and product yields in the heterogeneous reactions of HOBr with ice surfaces containing NaBr and NaCl". In: *The Journal of Physical Chemistry A* 106.21, pp. 5279–5287. DOI: 10.1021/jp014296m.

Jacob, Daniel (1999). *Introduction to atmospheric chemistry*. Princeton University Press.

Kaleschke, L et al. (2004). "Frost flowers on sea ice as a source of sea salt and their influence on tropospheric halogen chemistry". In: *Geophysical research letters* 31.16. DOI: 10.1029/2004GL020655.

Lacis, Andrew A et al. (1990). "Radiative forcing of climate by changes in the vertical distribution of ozone". In: *Journal of Geophysical Research: Atmospheres* 95.D7, pp. 9971–9981. DOI: 10.1029/JD095iD07p09971.

Liang, Q et al. (2010). "Finding the missing stratospheric Br y: a global modeling study of CHBr 3 and CH 2 Br 2". In: *Atmospheric Chemistry and Physics* 10.5, pp. 2269–2286.

Lund, Marianne T et al. (2014). "Global and regional climate impacts of black carbon and co-emitted species from the on-road diesel sector". In: *Atmospheric environment* 98, pp. 50–58.

Martinez, M et al. (1999). "The role of bromine and chlorine chemistry for arctic ozone depletion events in Ny-Ålesund and comparison with model calculations". In: *Annales Geophysicae*. Vol. 17. 7. Springer, pp. 941–956. DOI: 10.1007/s00585-999-0941-4.

Monitoring, Arctic et al. (2015). *AMAP Assessment 2015: Black carbon and ozone as Arctic climate forcers*. Arctic Monitoring and Assessment Programme (AMAP).

Monks, Paul S (2000). "A review of the observations and origins of the spring ozone maximum". In: *Atmospheric Environment* 34.21, pp. 3545–3561. DOI: 10.1016/S1352-2310(00)00129-1.

Monks, Paul Steven et al. (2015). "Tropospheric ozone and its precursors from the urban to the global scale from air quality to short-lived climate forcer". In: *Atmospheric Chemistry and Physics* 15.15, pp. 8889–8973.

Myhre, G. et al. (2013). *Anthropogenic and Natural Radiative Forcing. In: Climate Change 2013: The Physical Science Basis. Contribution of Working Group I to the Fifth Assessment Report of the Intergovernmental Panel on Climate Change [Stocker, T.F., D. Qin, G.–K. Plattner, M. Tignor, S.K. Allen, J. Boschung, A.Nauels, Y. Xia, V. Bex and P.M. Midgley (eds.)].* Cambridge University Press, Cambridge, United Kingdom and New York, NY, USA, pp. 659–740. DOI: doi:10.1017/CBO9781107415324.018.

Parrella, JP et al. (2012). "Tropospheric bromine chemistry: implications for present and pre-industrial ozone and mercury". In: *Atmospheric Chemistry and Physics* 12.15, pp. 6723–6740.

Parrish, DD et al. (2009). "Increasing ozone in marine boundary layer inflow at the west coasts of North America and Europe". In: *Atmospheric Chemistry and Physics* 9.4, pp. 1303–1323.

Parrish, DD et al. (2014). "Long-term changes in lower tropospheric baseline ozone concentrations: Comparing chemistry-climate models and observations at northern midlatitudes". In: *Journal of Geophysical Research: Atmospheres* 119.9, pp. 5719–5736. DOI: 10.1002/2013JD021435.

Prather, Michael J (1986). "Numerical advection by conservation of second-order moments". In: *Journal of Geophysical Research: Atmospheres* 91.D6, pp. 6671–6681. DOI: 10.1029/JD091iD06p06671.

— (2012). *Fast-JX version 6.7*. ftp://halo.ess.uci.edu/public/prather/Fast-J/.

Prather, Michael J et al. (2008). "Quantifying errors in trace species transport modeling". In: *Proceedings of the National Academy of Sciences* 105.50, pp. 19617–19621. DOI: 10.1073/pnas.0806541106.

Quack, Birgit et al. (2003). "Air-sea flux of bromoform: Controls, rates, and implications". In: *Global Biogeochemical Cycles* 17.1. DOI: 10.1029/2002GB001890.

Rankin, Andrew M et al. (2002). "Frost flowers: Implications for tropospheric chemistry and ice core interpretation". In: *Journal of Geophysical Research: Atmospheres* 107.D23. DOI: 10.1029/2002JD002492.

Röth, Ernst-Peter (1992). "A fast algorithm to calculate the photonflux in optically dense media for use in photochemical models". In: *Berichte der Bunsengesellschaft für physikalische Chemie* 96.3, pp. 417–420. DOI: 10.1002/bbpc.19920960335.

— (2002). *Description of the anisotropic radiation transfer model ART to determine photodissociation coefficients*. Forschungszentrum, Zentralbibliothek.

Sand, M et al. (2012). "The Arctic response to remote and local forcing of black carbon." In: *Atmospheric Chemistry & Physics Discussions* 12.7. DOI: 10.5194/acp-13-211-2013.

Sander, SP et al. (2006). *Chemical kinetics and photochemical data for use in atmospheric studies evaluation number 15*. Tech. rep. Pasadena, CA: Jet Propulsion Laboratory, National Aeronautics and Space Administration, 2006.

Schwartz, Stephen E (1986). "Mass-transport considerations pertinent to aqueous phase reactions of gases in liquid-water clouds". In: *Chemistry of multiphase atmospheric systems*. Springer, pp. 415–471. DOI: 10.1007/978-3-642-70627-1_16.

Seinfeld John, H (1988). "Pandis and Spyros N". In: *Atmospheric Chemistry and Physics—From Air Pollution to Climate Change. John Wiley and Sons, Inc*.

Shaw, PM et al. (2010). "Arctic organic aerosol measurements show particles from mixed combustion in spring haze and from frost flowers in winter". In: *Geophysical Research Letters* 37.10. DOI: 10.1029/2010GL042831.

Sherwen, Tomás et al. (2017). "Halogen chemistry reduces tropospheric O 3 radiative forcing". In: *Atmospheric Chemistry and Physics* 17.2, pp. 1557–1569. DOI: 10.5194/acp-17-1557-2017.

Shindell, Drew et al. (2009). "Climate response to regional radiative forcing during the twentieth century". In: *Nature Geoscience* 2.4, pp. 294–300. DOI: 10.1038/NGEO473.

Simpson, William R et al. (2015). "Tropospheric halogen chemistry: Sources, cycling, and impacts". In: *Chemical reviews* 115.10, pp. 4035–4062.

Simpson, WR et al. (2007). "Halogens and their role in polar boundary-layer ozone depletion". In: *Atmospheric Chemistry and Physics* 7.16, pp. 4375–4418. DOI: 10.5194/acp-7-4375-2007.

Søvde, Ole Amund (2016). "Oslo CTM3 v0.9 User Manual". In:

Søvde, Ole Amund et al. (2012). "The chemical transport model Oslo CTM3". In: *Geoscientific Model Development* 5.6. DOI: 10.5194/gmd-5-1441-2012.

Stevenson, DS et al. (2006). "Multimodel ensemble simulations of present-day and near-future tropospheric ozone". In: *Journal of Geophysical Research: Atmospheres* 111.D8. DOI: 10.1029/2005JD006338.

Stevenson, DS et al. (2013). "Tropospheric ozone changes, radiative forcing and attribution to emissions in the Atmospheric Chemistry and Climate Model Intercomparison Project (ACCMIP)". In: *Atmospheric Chemistry and Physics* 13.6, pp. 3063–3085. DOI: 10.5194/acp-13-3063-2013.

Vingarzan, Roxanne (2004). "A review of surface ozone background levels and trends". In: *Atmospheric Environment* 38.21, pp. 3431–3442. DOI: 10.1016/j.atmosenv.2004.03.030.

Ziska, Franziska et al. (2013). "Global sea-to-air flux climatology for bromoform, dibromomethane and methyl iodide". In: *Atmospheric Chemistry and Physics* 13.17, pp. 8915–8934. DOI: 10.5194/acp-13-8915-2013.